

Human Monoclonal Antibodies Broadly Neutralizing against Influenza B Virus

Mayo Yasugi^{1,2,3}, Ritsuko Kubota-Koketsu^{1,3,4}, Akifumi Yamashita⁵, Norihito Kawashita⁶, Anariwa Du^{1,3}, Tadahiro Sasaki^{1,3}, Mitsuhiro Nishimura^{1,3}, Ryo Misaki^{3,7}, Motoki Kuhara^{3,8}, Naphatsawan Boonsathorn^{3,9}, Kazuhito Fujiyama^{3,7}, Yoshinobu Okuno⁴, Takaaki Nakaya^{3,10*}, Kazuyoshi Ikuta^{1,3*}

1 Department of Virology, Research Institute for Microbial Diseases (RIMD), Osaka University, Suita, Osaka, Japan, **2** Graduate School of Life and Environmental Sciences, Osaka Prefecture University, Izumisano, Osaka, Japan, **3** The Japan Science and Technology Agency/Japan International Cooperation Agency, Science and Technology Research Partnership for Sustainable Development (JST/JICA, SATREPS), Tokyo, Japan, **4** Kanonji Institute, The Research Foundation for Microbial Diseases of Osaka University, Kanonji, Kagawa, Japan, **5** Department of Genome Informatics, RIMD, Osaka University, Suita, Osaka, Japan, **6** Department of Environmental Pharmacometrics, Graduate School of Pharmaceutical Sciences, Osaka University, Suita, Osaka, Japan, **7** Applied Microbiology Laboratory, International Center of Biotechnology, Osaka University, Suita, Osaka, Japan, **8** Ina Laboratory, Medical & Biological Laboratories Corporation, Ltd., Ina, Nagano, Japan, **9** Department of Medical Sciences, Ministry of Public Health, Muang, Nonthaburi, Thailand, **10** International Research Center for Infectious Diseases (RIMD), Osaka University, Suita, Osaka, Japan

Abstract

Influenza virus has the ability to evade host immune surveillance through rapid viral genetic drift and reassortment; therefore, it remains a continuous public health threat. The development of vaccines producing broadly reactive antibodies, as well as therapeutic strategies using human neutralizing monoclonal antibodies (HuMAbs) with global reactivity, has been gathering great interest recently. Here, three hybridoma clones producing HuMAbs against influenza B virus, designated 5A7, 3A2 and 10C4, were prepared using peripheral lymphocytes from vaccinated volunteers, and were investigated for broad cross-reactive neutralizing activity. Of these HuMAbs, 3A2 and 10C4, which recognize the readily mutable 190-helix region near the receptor binding site in the hemagglutinin (HA) protein, react only with the Yamagata lineage of influenza B virus. By contrast, HuMAb 5A7 broadly neutralizes influenza B strains that were isolated from 1985 to 2006, belonging to both Yamagata and Victoria lineages. Epitope mapping revealed that 5A7 recognizes 316G, 318C and 321W near the C terminal of HA1, a highly conserved region in influenza B virus. Indeed, no mutations in the amino acid residues of the epitope region were induced, even after the virus was passaged ten times in the presence of HuMAb 5A7. Moreover, 5A7 showed significant therapeutic efficacy in mice, even when it was administered 72 hours post-infection. These results indicate that 5A7 is a promising candidate for developing therapeutics, and provide insight for the development of a universal vaccine against influenza B virus.

Citation: Yasugi M, Kubota-Koketsu R, Yamashita A, Kawashita N, Du A, et al. (2013) Human Monoclonal Antibodies Broadly Neutralizing against Influenza B Virus. *PLoS Pathog* 9(2): e1003150. doi:10.1371/journal.ppat.1003150

Editor: Veronika von Messling, Paul-Ehrlich-Institut, Germany

Received: July 17, 2012; **Accepted:** December 7, 2012; **Published:** February 7, 2013

Copyright: © 2013 Yasugi et al. This is an open-access article distributed under the terms of the Creative Commons Attribution License, which permits unrestricted use, distribution, and reproduction in any medium, provided the original author and source are credited.

Funding: This work was supported in part by the Japan Science and Technology Agency/Japan International Cooperation Agency, Science and Technology Research Partnership for Sustainable Development (JST/JICA, SATREPS) (http://www.jst.go.jp/global/kadai/h2011_thailand.html); and a Grant-in-Aid for Young Scientists (B) from the Japan Society for the Promotion of Science to M.Y. (#23790660). Also the funders had no role in study design, data collection and analysis, decision to publish, or preparation of the manuscript.

Competing Interests: The authors have declared that no competing interests exist.

* E-mail: ikuta@biken.osaka-u.ac.jp

‡ Current address: Department of Infectious Diseases, Kyoto Prefectural University of Medicine, Kamigyo-ku, Kyoto, Japan.

Introduction

Influenza virus remains a constant public health threat. During annual epidemics 5–15% of the worldwide population are typically infected, resulting in 3 to 5 million cases of severe illness and between 250,000 to 500,000 deaths per year [1,2]. While all age groups are affected by the disease, most influenza-related hospitalizations in industrialized countries occur in young children, the elderly, and the immunocompromised [3]. Like H1 and H3 subtypes of influenza A virus, influenza B virus also causes epidemics in humans [2]. In contrast to influenza A virus, influenza B virus is found almost exclusively in humans and has a much slower mutational rate [3–5]. However, cocirculation of two phylogenetically and antigenically distinct lineages, represented by

B/Yamagata/16/1988 and B/Victoria/2/1987, has caused antigenic variation through genetic reassortment and antigenic drift from cumulative mutations, leading to annual epidemics [6,7].

Currently, two main countermeasures, vaccines and antiviral drugs, are used against influenza virus [8]. Vaccination has been the mainstay of infection control. However, the protection afforded by vaccination varies widely, depending on the antigenic match between the viral strains in the vaccine and those that are circulating during a given influenza season, as well as on the recipient's age and health status [1,3,9]. Neuraminidase inhibitors, such as oseltamivir (Tamiflu) and zanamivir (Relenza), and matrix 2 (M2) ion channel inhibitors like amantadine, have been widely used for the treatment of influenza viral infection and are proven to be quite effective against susceptible strains [10]. However, they

Author Summary

Influenza virus is classified into types A, B and C. Influenza A virus is further divided into many subtypes, all of which exist in animals, indicating pandemic potential. By contrast, influenza B virus circulates almost exclusively in humans and, as there is no evidence for reassortment with influenza A virus, there is no indication of pandemic potential. Hence, there is far less accumulated research information regarding influenza B virus than influenza A virus. Influenza B virus, which is classified into two phylogenetic lineages, does, however, cause annual epidemics in humans and is therefore as essential to control as influenza A virus. Recently, the development of a universal vaccine and therapeutic strategies using human monoclonal antibodies (HuMAbs) has been gathering great interest. The present study reports a HuMAb neutralizing a wide range of influenza B viruses of both lineages. This HuMAb recognizes the conserved region of hemagglutinin. Moreover, therapeutic efficacy of this HuMAb was also confirmed by *in vivo* animal experiments. Thus, this study provides insight for the development of broad-spectrum therapeutics and a universal prophylactic vaccine against influenza B virus.

have limited efficacy in delayed administration after the onset of illness [11], and widespread use has resulted in the emergence of resistant viral strains, as seen in H1N1 and H3N2 [12–15]. Of note, M2 blockers are not active against influenza B virus as it has no equivalent to the M2 ion channel protein of influenza A virus [16]. Thus, the development of therapeutic approaches and vaccine design that provide potent and broadly cross-protective host immunity are a global public health priority [17].

Human monoclonal antibodies (HuMAbs) prepared from vaccinated donors and patients with viral infections could have potential therapeutic application, and provide significant information on human epitopes that could be important for developing the next generation of universal vaccines [18,19]. In addition to classical hybridoma methods [20], recent advances in technology, such as transgenic mice [21] and yeast or phage display [22,23], have renewed interest in the development of HuMAbs [17,24,25]. Thus, using phage display or single cell culture methods, several HuMAbs with broad neutralizing activities have been identified against the hemagglutinin (HA) protein in influenza A viruses, including C6261 and F10 which react with group 1 [26,27], and CR8020 which reacts with group 2 viruses [28]. Another HuMAb, FI6v3, that neutralizes both group 1 and group 2 influenza A viruses, has also recently been described [29]. For influenza B virus, by contrast, broadly neutralizing HuMAbs, CR8033, CR8071 and CR9114, have firstly reported on September 2012 [30].

A hybridoma method for establishing HuMAbs was developed previously in this laboratory by fusion of the peripheral blood mononuclear cells (PBMCs) of influenza-vaccinated healthy volunteers with the fusion partner cell line SPYMEG, which has been optimized for higher reliability of cell fusion by overcoming chromosome deletion problem [31,32]. In this study, three HuMAbs that neutralize influenza B virus were prepared using this method. One of the three HuMAbs, 5A7, reacted broadly with influenza B virus isolates from 1985 to 2006 that belong to both the Yamagata and Victoria lineages, and recognized a highly conserved region in the HA protein. Moreover, 5A7 showed therapeutic efficacy even in mice treated with the HuMAb 72 hours post-infection. These results indicate that 5A7 is a

promising candidate for developing therapeutics and will provide insight for the development of the next generation of vaccines universally effective against influenza B virus.

Results

Preparation of anti-influenza B HuMAbs

Healthy volunteers were vaccinated with the trivalent HA split vaccine including A/Brisbane/59/2007 (H1N1), A/Uruguay/716/2007 (H3N2), and B/Florida/4/2006 strains. Then, 1–2 weeks later, the vaccine-derived PBMCs were fused with SPYMEG cells. After screening for MAb specificity to influenza viruses, the cells in the specific MAb-positive wells were cloned by limiting dilution. Ultimately, three hybridoma clones producing HuMAbs, designated 5A7, 3A2 and 10C4, were established against influenza B virus. These HuMAbs did not react with influenza A virus. HuMAb reactivity was tested by immunofluorescence assay (IFA) and western blotting using Madin-Darby canine kidney (MDCK) cells infected with B/Florida/4/2006, homologous with the vaccine antigen. All three HuMAbs reacted with HA protein expressed by transfection into 293T cells (Table S1). IgG isotyping was performed by ELISA and revealed that HuMAbs 5A7 and 10C4 were IgG1, and 3A2 was IgG3 (Table S1). Sequences of the V_H and V_L region of the three HuMAbs were compared and analyzed to the closest germline sequences using IgBlast software in NCBI database. These three HuMAbs were derived from different germ lines except D region in V_H of 3A2 and 10C4 (Figure 1).

Neutralizing activities of HuMAbs

Next, the three HuMAbs were evaluated for their ability to neutralize influenza B viruses by *in vitro* virus neutralization (VN) assay (Figure 2). The VN test was carried out on MDCK cells infected with influenza B virus under the treatment with serial four-fold dilutions of HuMAbs. The viruses used were B/Florida/4/2006, B/Shanghai/361/2002, B/Johannesburg/5/1999, B/Yamanashi/166/1998 and B/Mie/1/1993 for the Yamagata lineage, and B/Malaysia/2506/2004, B/Shandong/7/1997 and B/Victoria/2/1987 for the Victoria lineage. The mouse-adapted B/Ibaraki/2/1985 in the Victoria lineage, used in the passive transfer experiment described below, was also subjected to VN assay. HuMAb 5A7 showed a lower neutralizing activity compared with 3A2 and 10C4 against the Yamagata lineage; however, 5A7 neutralized all strains in the Yamagata and Victoria lineages that were isolated during 1985 to 2006. HuMAbs 3A2 and 10C4 neutralized the Yamagata lineage effectively, whereas they had little neutralization effect on all the Victoria lineage viruses. An anti-dengue virus HuMAb (D23-1B3B9) derived from PBMCs of a patient infected with dengue virus serotype 2 [33] was used as a control IgG. It did not neutralize any influenza B viral strains.

To clarify the mechanism of neutralization by the three HuMAbs, hemagglutinin inhibition (HI) and fusion inhibition assays were performed. All three HuMAbs had HI activity; 3A2 and 10C4 showed markedly higher HI titers (0.39 $\mu\text{g/ml}$) than 5A7 (25.0 $\mu\text{g/ml}$). Fusion inhibition assay showed that they all had the ability to inhibit cell-cell fusion; the concentration of HuMAb necessary for complete inhibition was lower for 3A2 and 10C4 (25 $\mu\text{g/ml}$) than 5A7 (100 $\mu\text{g/ml}$) at pH 5.5 (Figure S1). By contrast, the control IgG did not show any HI or fusion inhibition activity, even at 100 $\mu\text{g/ml}$.

In addition, HuMAbs 5A7, 3A2 and 10C4 were subjected to surface plasmon resonance analysis to examine their binding affinities. Each HuMAb was immobilized on the surface of the

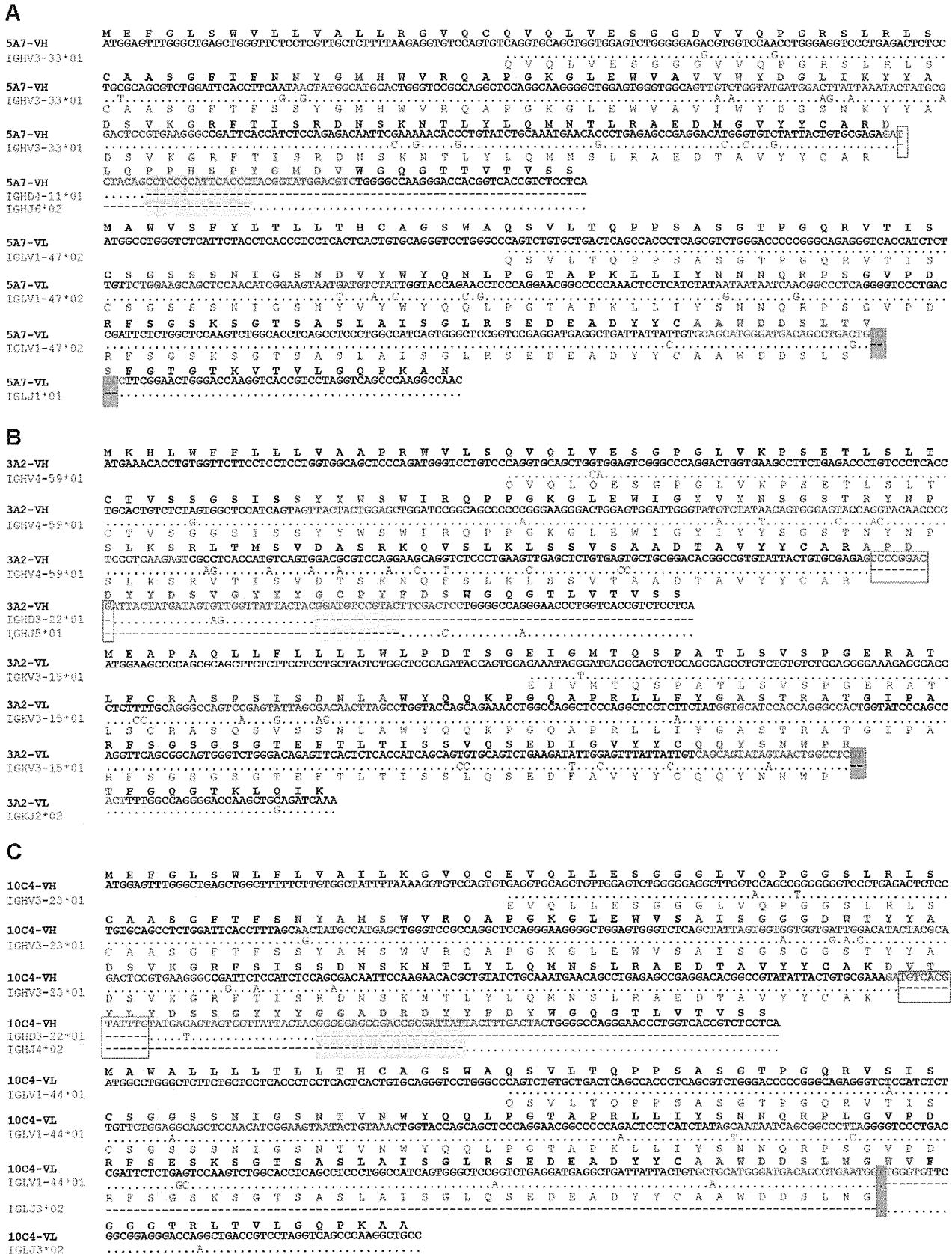


Figure 1. Nucleotide and amino acid sequences of the V_H and V_L of three HuMAbs 5A7 (A), 3A2 (B) and 10C4 (C). Closest germline sequences in NCBI database by IgBlast softwares were aligned. Complementarity-determining regions (CDRs) are indicated in red, blue and pink (CDRs 1, 2 and 3, respectively). V-D and D-J junctions in VH and V-J junctions in VL are shown in white, light gray and dark gray colors, respectively. doi:10.1371/journal.ppat.1003150.g001

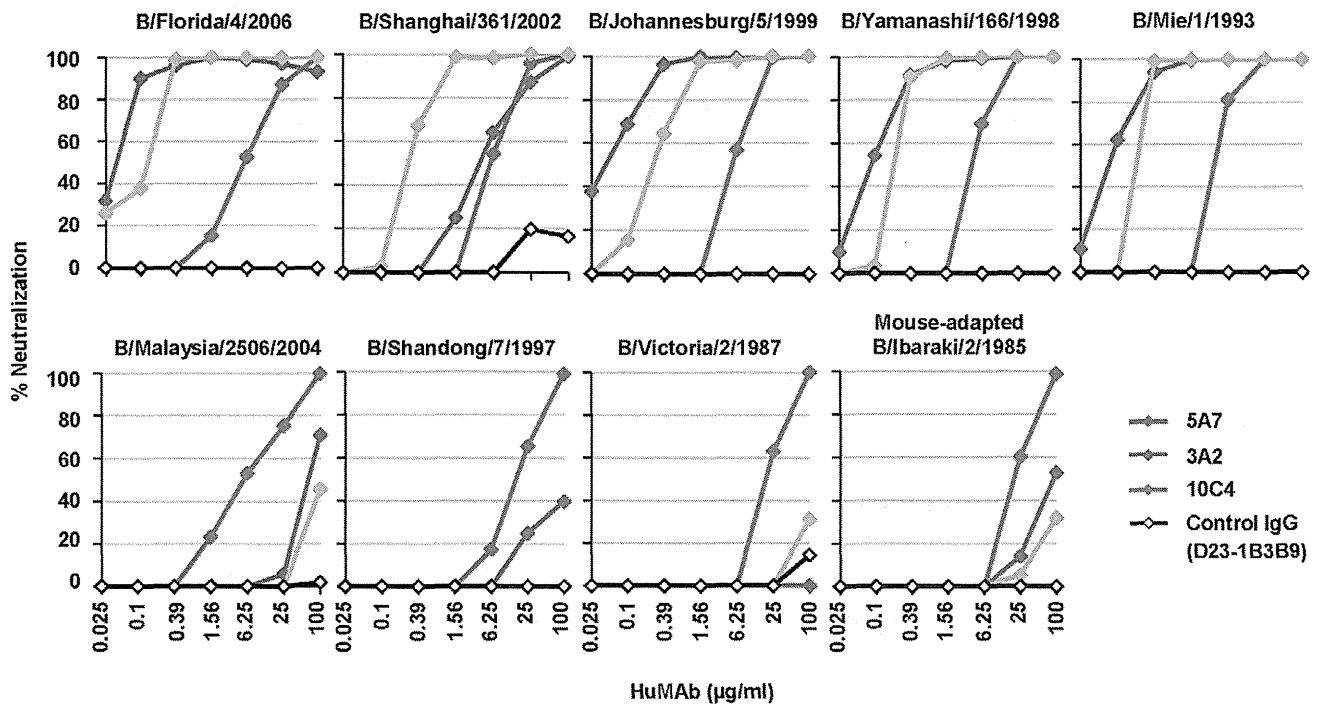


Figure 2. Reactivity of three HuMAbs. *In vitro* VN assay was performed with HuMAbs 5A7 (red), 3A2 (blue), 10C4 (green) and control IgG (D23-1B3B9; black). HuMAbs (100 µg/ml) were serially four-fold diluted. The percentage of neutralization was estimated as the viral infectivity under HuMAb-treated conditions compared with that without HuMAb. Upper panels are Yamagata lineage viruses and lower panels are Victoria lineage viruses.

doi:10.1371/journal.ppat.1003150.g002

sensor chip. The vaccine antigen, HA protein of B/Florida/4/2006, at concentrations 12.5, 25, 50, 100 and 200 nM was consecutively injected on the chip surface and the association and dissociation phases were monitored. K_D value could not be calculated for 5A7 precisely as it was difficult to dissociate from HA (Table 1 and Figure S2). However, the estimated K_D value of 5A7 (less than 5.6×10^{-9} M) was similar to that of 10C4 (1.8×10^{-9} M). By contrast, the control IgG did not associate with HA at all (data not shown).

Epitope mapping of three HuMAbs

Next, the epitope regions recognized by the three HuMAbs were determined. At first, escape mutants were selected by culturing B/Florida/4/2006 in the presence of serial ten-fold diluted HuMAb. MDCK cells were infected with the mixture in a 24-well plate and 72 hours later the supernatants were subjected to VN and HI assays, and direct sequencing analysis of the HA gene (Figure S3). Escape mutants were not established for 5A7,

even after the virus was serially passed 10 times in the presence of this HuMAb. 5A7 reacted with the HA protein by western blotting under reducing conditions. Therefore, the region of 5A7 involved in recognition was refined using HA truncation vectors containing HA segments of varying length (Figure 3A). Western blotting with 5A7 was carried out on 293T cells transfected with the truncated HA expression vectors. HuMAb 5A7 reacted with truncated HA segments that included amino acid residues 1–324 but not with those with residues 1–314 (Figure 3A); amino acid numbering was started after the signal peptide [34]. These results indicate that 5A7 recognizes amino acid residues between 315 to 324 (IGNCPIWVKT) in the HA protein, which locates near the C terminal of the HA1 protein. The epitope region of 5A7 was determined by mutating each of the 315–324 amino acid residues singly. Each residue was replaced by alanine using a site-directed mutagenesis method. Mutant HAs expressed in 293T cells were tested for reactivity with 5A7 by IFA. Mutants G316A, C318A and W321A did not react with 5A7 (Figure 3B), indicating that 316G, 318C and 321W amino acids critically affected the structure of the epitope of 5A7. To estimate the conservation of the amino acid sequences in the epitope of 5A7, HA sequences of influenza B virus were extracted from the NCBI database. Notably, 2,851 among 2,853 viral sequences (99.93%) showed an identical amino acid sequence in the epitope region (Table S2). Among the Yamagata and Victoria lineages, there was only 1 divergent strain, respectively.

By contrast, escape mutants were obtained in the presence of 3A2 and 10C4. They showed four-fold reduced VN and HI activities compared with the parent virus after just one passage of the virus (Figure S3). Each escape mutant obtained in the presence of 3A2 and 10C4 had amino acid substitutions at identical positions, 194D and 196T (Figure S4), both located in the readily

Table 1. Kinetic constants of HuMAbs binding to influenza B virus-derived HA.

	k_{on}^1 (S^{-1})	k_{off}^2 ($M^{-1}S^{-1}$)	K_D (M)
5A7	1.8×10^3	$< 1.0 \times 10^{-5}$	$< 5.6 \times 10^{-9}$
3A2	5.3×10^4	2.1×10^{-5}	4.0×10^{-10}
10C4	1.6×10^4	2.8×10^{-5}	1.8×10^{-9}

¹Association rate constant.

²Dissociation rate constant.

doi:10.1371/journal.ppat.1003150.t001

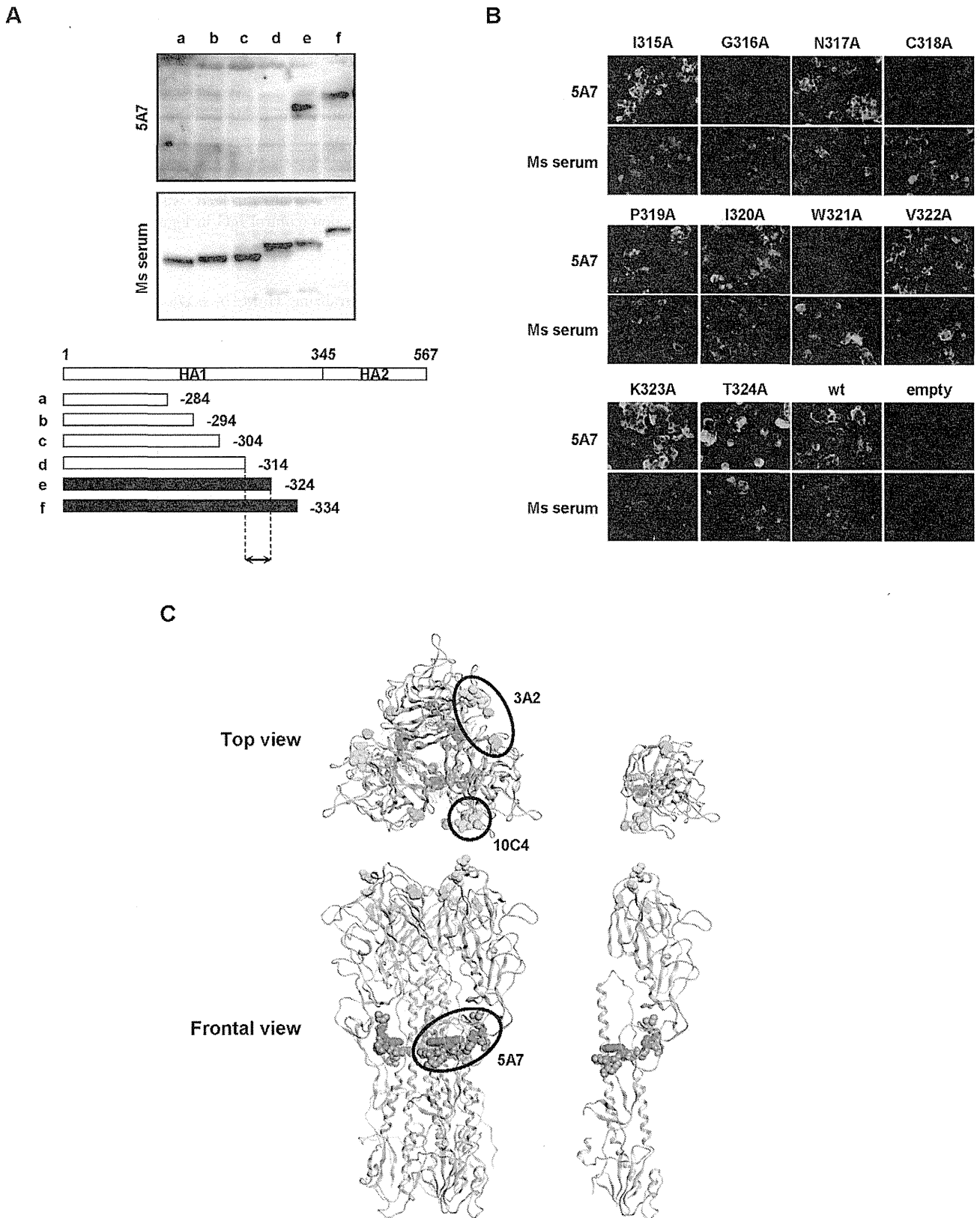


Figure 3. Epitope mapping of HuMAbs. (A) Reactivity of 5A7 with truncated HA. A series of truncated forms of HA (a to f) were prepared in an expression plasmid as depicted in the diagram. Transfected 293T cells were subjected to western blotting with 5A7 or serum from a mouse infected with B/ibaraki/2/1985 as a control (Ms serum). Black bars in the HA diagram indicate reactivity with 5A7. Arrowed region is the estimated region involved in recognition. (B) Expression plasmids bearing one point mutated B/Florida/4/2006 HA protein were prepared. 293T cells expressing the mutated HA were subjected to IFA with 5A7 (upper panels) or Ms serum as a control (lower panels). Wild type B/Florida/4/2006 (wt) and pCAGGSII

vector without an insertion (empty) were used as controls. (C) Epitope map of the HuMAbs in the three-dimensional structure of the HA trimer (left models) and monomer (right models). The amino acid positions identified by epitope mapping are 315 to 324 (dark yellow), 316, 318 and 321 (pink), 194 and 196 (blue), 131 and 227 (green). The epitope region of each HuMAb is circled. doi:10.1371/journal.ppat.1003150.g003

mutable 190-helix antigenic site near the receptor binding site [34]. In addition, the different amino acid residues in V_H and V_L of 3A2 and 10C4 (Figure 1) indicated that these two HuMAbs were derived from different germ lines. These results are consistent with 3A2 and 10C4 reactivity with only the Yamagata strains, since Yamagata and Victoria strains differ in amino acid sequence at this position. HuMAb 3A2 showed low reactivity against B/Shanghai/361/2002 (Figure 2A) and was therefore examined for an additional distinct epitope region. To do this, various chimeric sequences of HA were constructed from B/Florida/4/2006 and B/Shanghai/361/2002, which differ at seven residues (positions 37, 40, 88, 131, 227, 249 and 456), expressed in plasmids, and transfected into 293T cells. IFA of the chimeric HA proteins expressed in 293T cells showed that 131P and 227S were essential for reaction with 3A2 (Figure S5). These results indicate that the epitope of 3A2 is dependent on residues at positions 131, 194, 196 and 227, and the epitope of 10C4 is dependent on residues at positions 194 and 196.

The epitope regions to which the three HuMAbs map are shown in an HA monomer and trimer three-dimensional models in Figure 3C. HuMAbs 3A2 and 10C4 recognized the top of the globular head including the 190-helix antigenic site, whereas 5A7 reacted with the stalk region distant from the viral membrane.

Therapeutic efficacy of 5A7 *in vivo*

The evaluation of 5A7 as a passive transfer therapy for influenza B viral infection was examined in mice. Six-week-old mice were treated intraperitoneally with 5A7 at 1, 5, 10 or 15 mg/kg or with control IgG at 10 mg/kg, 4 hours after an intranasal injection with a lethal dose (1.47×10^3 50% mouse lethal dose (MLD₅₀/mouse) of mouse-adapted B/Ibaraki/2/1985. Survival rate and body weight change were checked daily. When body weight decreased to less than 60% of starting weight, mice were sacrificed. With respect to survival rate, complete therapeutic efficacy against the virus challenge was seen with 5, 10 and 15 mg/kg of 5A7 examined (Figure 4A, Upper panel). The weight change was mild in the groups, especially in those treated with 5A7 at 10 or 15 mg/kg (Figure 4A, lower panel).

Next, viral load in the lungs was titrated. Mice infected with mouse-adapted B/Ibaraki/2/1985 (1.47×10^3 MLD₅₀/mouse), or B/Florida/4/2006 that had been passaged eight times in mice lungs (5.0×10^3 focus-forming units (FFU)/mouse), were treated with 5A7 or control IgG at 10 mg/kg 4 hours post-infection, and then sacrificed on day 3 and day 6 post-infection. The lungs were homogenized and tested in focus-forming assays with MDCK cells. The viral titers were significantly lower in 5A7-treated mice compared to the control IgG-treated group for both viral infections (Figure 4B). Finally, mice were treated with 5A7 or control IgG at 10 mg/kg intraperitoneally at 4, 24, 48 or 72 hours after an intranasal injection with a lethal dose (1.47×10^3 MLD₅₀/mouse) of mouse-adapted B/Ibaraki/2/1985. Survival rate and body weight change were monitored (Figure 4C). Two independent experiments were similarly performed for 5A7 treatment with five mice/group/experiment (Experiments 1 and 2 in Figure 4C). When administered 4 hours post-infection, 5A7 treatment showed complete therapeutic efficacy, as was observed above (shown in Figure 4A). Notably, 80% of mice were alive in the group treated with 5A7 24 hours post-infection. Moreover, several mice survived after treatment with 5A7 48 hours post-infection and, surprisingly,

more mice survived when treated 72 hours post-infection. By contrast, 80% of mice treated with control IgG at 4 hours post-infection died and the surviving 20% did not show recovery of body weight during the experiment. All of mice died by 8 days post-infection in the groups treated with control IgG after 24 hours post-infection (control IgG in Figure 4C).

Discussion

A broadly neutralizing HuMAb, 5A7, was established using PBMC from a vaccinated healthy volunteer. This antibody neutralizes influenza B virus strains isolated between 1985 and 2006 that belong to the Yamagata or Victoria lineage. Moreover, therapeutic efficacy was shown in mice even when the HuMAb was administered 48 or 72 hours after viral challenge. As previously reported for almost all MAbs broadly neutralizing influenza virus, 5A7 recognized the stalk region of the HA protein [26–29]. Importantly, the epitope region recognized by 5A7 is highly conserved in influenza B virus and the divergent strains occur only sparsely (Table S2). Although influenza B virus has a much slower mutational rate than that observed for influenza A subtypes like H1 and H3, cocirculation of two phylogenetically and antigenically distinct lineages of influenza B virus leads to annual epidemics in humans [6,7]. Dreyfus *et al.* first reported broadly neutralizing HuMAbs against influenza B virus in September 2012 [30]. The epitope regions they identified were distinct from that of our HuMAb, 5A7. Characterization of the epitope region recognized by such a HuMAb could therefore provide insight for the development of a universal vaccine.

The high degree of conservation of amino acid residues in the epitope region implies that influenza B virus would not easily induce mutation in this region. Indeed, amino acid residues in the epitope region did not mutate even when the virus was passaged ten times under 5A7-treatment conditions. It could be considered that the poor inhibitory activity of 5A7 (weak HI, fusion inhibition and VN₅₀) is the cause of failure to establish escape mutants. However, a previous report showed that escape mutants could be prepared even from an MAb with weak fusion inhibition and complete neutralizing activities (25 and 50 µg/ml, respectively), and without HI activity, in order to map its epitope [35,36]. Since 5A7 shows similarly weak activity, we would also expect to have been able to prepare 5A7 escape mutants and determine the epitope region. Failure to establish escape mutants in the presence of 5A7 could be an advantage for its development as a therapeutic tool, and also for designing the next generation of globally effective vaccines.

Generally, MAbs recognizing the globular head show strong HI activity, whereas those against the stalk region usually show none [35]. Thus, it is considered that MAbs against the globular head inhibit the receptor binding step, while MAbs against the stalk region inhibit the fusion step, in viral replication [26,37]. In fact, HuMAbs, 3A2 and 10C4, that recognize the 190-helix in the globular head near the receptor binding site, showed strong HI activity, which suggests that they can inhibit viral binding to the receptor on the host cells. Their ability to inhibit the fusion process (Figure S1) implies that they could secondarily disturb the low pH-dependent structural change in HA by binding to the globular head. Surprisingly, although 5A7 reacted to the stalk region it also showed specific and weak HI activity. This suggests that MAb

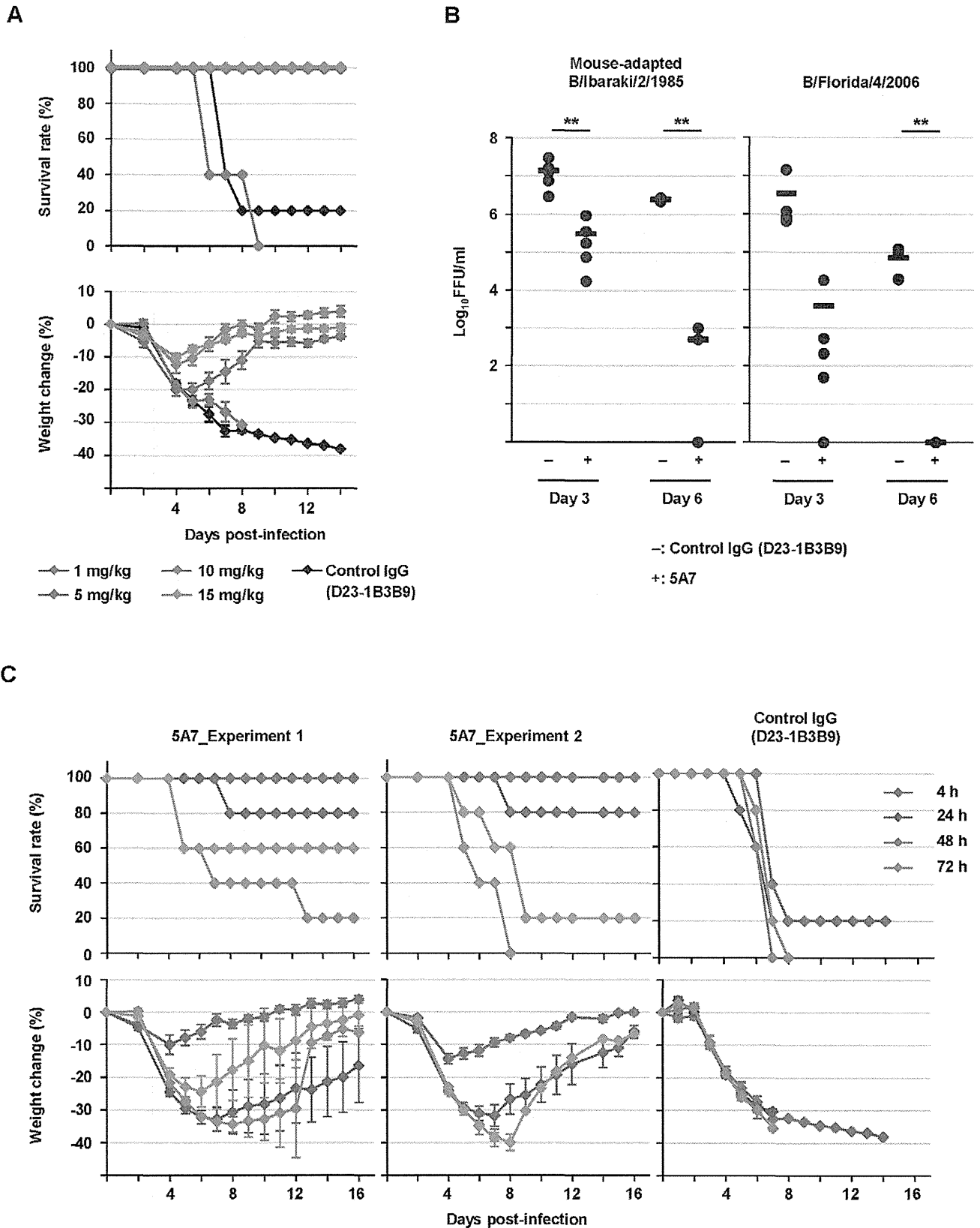


Figure 4. Therapeutic efficacy of 5A7 in mice. (A) Mice were treated intraperitoneally with HuMAb 5A7 at 1 (red line), 5 (blue), 10 (green), or 15 (orange) mg/kg or with control IgG at 10 mg/kg (black) 4 hours after intranasal injection of a lethal dose (1.47×10^3 MLD₅₀/mouse) of mouse-adapted B/ibaraki/2/1985. Survival and body weight were checked daily. Each group consists of five mice. Body weight is shown as the mean \pm SEM of five mice. (B) Mice were treated with 5A7 (+) or control IgG (D23-1B3B9; -) at 10 mg/kg 4 hours post-infection with 1.47×10^3 MLD₅₀/mouse of mouse-adapted B/ibaraki/2/1985 (left panel) or 5.0×10^3 FFU/mouse of B/Florida/4/2006 passaged eight times in mouse lung (right panel). The titers in lungs

were calculated at day 3 and day 6 post-infection. Each group consists of five mice (except control IgG-treated group with mouse-adapted B/Ibaraki/2/1985 at day 6, which consists of four mice as one accidentally died before the lung could be collected). Black bars are mean values. **: $P < 0.01$ compared to control IgG-treated group. (C) Two independent experiments were similarly performed (Left two panels). Mice were given 10 mg/kg HuMAb 5A7 at 4 (red line), 24 (blue), 48 (green) or 72 (orange) hours post-infection with mouse-adapted B/Ibaraki/2/1985 (1.47×10^3 MLD₅₀/mouse). Right panel shows 10 mg/kg control IgG-treated group at 4, 24, 48 or 72 hours post-infection. Survival and body weight were checked daily. Each group consists of five mice per experiment. Body weight is shown as the mean \pm SEM of five mice. doi:10.1371/journal.ppat.1003150.g004

recognizing the stalk region distal from the viral membrane could affect the ability of the virus to bind to the receptor. As reported for MAbs reacting to the stalk region, 5A7 also showed specific fusion inhibition activity [28,38]. These results suggest that HuMAb 5A7 could inhibit viral entry by preventing receptor binding, and the subsequent fusion process.

Previous reports show that the concentration of MAbs necessary for viral neutralization was much higher for those recognizing the stalk region of the envelope protein than for those reacting with the globular head in influenza viruses [28,36,39], as well as other viruses [40]. In agreement with these reports, the concentration required for viral neutralization in this study was higher for 5A7 than 3A2 and 10C4 (Figure 2). Such results can be explained by either a difference in binding affinity or in physical accessibility of HuMAbs to the epitope region. 5A7 showed similar K_D with 10C4 in binding kinetics analysis (Table 1 and Figure S2), indicating that 5A7 has more difficulty physically accessing the epitope region of the HA protein. Modifying the HuMAb structure to enable easier access to the epitope region and improving its binding affinity, as described [41,42], could lead to the development of better therapeutic HuMAbs for influenza.

HuMAb 5A7 had specific therapeutic efficacy in mice even when administered after viral challenge (Figure 4C). Two independent passive transfer experiments were performed. Surprisingly, in both experiments, mice treated with 5A7 HuMAb 72 hours post-infection had a better survival rate than those treated 48 hours post-infection. It is reported that in the first 24 hours after infection, the levels of lymphocyte apoptosis increase transiently in both nasal-associated lymphoid tissue and spleen, and cellular immune suppression occurs [43]. Temporal cellular immune suppression or infection-mediated endogenous signals could therefore interfere with the efficacy of exogenous HuMAb. These results imply that the timing of HuMAb treatment could be critical for efficacy, and therefore, injection at several time points may be necessary.

Mouse-adapted B/Ibaraki/2/1985 was used to examine the kinetics of survival rate and body weight change in passive transfer experiments because other viral strains are not lethal to mice, even if passaged several times *in vivo*. HuMAb 5A7 protected mice against mouse-adapted B/Ibaraki/2/1985 viral challenge although 5A7 was obtained from a volunteer vaccinated with B/Florida/4/2006 and had shown the lowest sensitivity to this viral strain *in vitro* (Figure 2). These results suggested that 5A7 would have therapeutic efficacy against a wide spectrum of influenza B viruses and, in fact, lung viral titers of both mouse-adapted B/Ibaraki/2/1985 and B/Florida/4/2006 were reduced significantly under 5A7-treatment conditions (Figure 4B). Further study using both mice and ferrets with several viral strains is needed to confirm the wide-ranging therapeutic potential of 5A7 *in vivo*.

Materials and Methods

Ethics statement

Human materials were collected using protocols approved by the Institutional Review Boards of the Research Institute for Microbial Diseases, Osaka University (#19-8-6). Written informed consent was obtained from the participants. Animal studies were

conducted under the applicable laws and guidelines for the care and use of laboratory animals in the Research Institute for Microbial Diseases, Osaka University. They were approved by the Animal Experiment Committee of the Research Institute for Microbial Diseases, Osaka University (#H21-24-0), as specified in the Fundamental Guidelines for the Proper Conduct of Animal Experiment and Related Activities in Academic Research Institutions under the jurisdiction of the Ministry of Education, Culture, Sports, Science and Technology, Japan, 2006.

HuMAb preparation

HuMAbs were prepared as described previously [31]. Briefly, 10 ml blood was drawn from a healthy volunteer vaccinated in the 2008/2009 winter season with trivalent HA split vaccine, which included A/Brisbane/59/2007, A/Uruguay/716/2007, and B/Florida/4/2006 (The Research Foundation for Microbial Diseases of Osaka University, Osaka, Japan), and PBMCs were collected by density gradient centrifugation through Ficoll-Paque Plus (GE Healthcare). SPYMEG cells were used as fusion partner cells. SPYMEG cells, which are non-secretors of human and murine immunoglobulins, were established by fusion between mouse myeloma cell line SP2/0-Ag14 and human megakaryoblastic cell line MEG-01 [31]. The PBMCs were fused with SPYMEG cells using polyethylene glycol #1500 (Roche). The fused cells were cultured in Dulbecco's modified Eagle medium (DMEM; Invitrogen) supplemented with 15% fetal bovine serum and hypoxanthine-aminopterin-thymidine. The first screening for antibody specificity to influenza virus was performed by IFA. Cells in the specific MAB-positive wells were then cloned by limiting dilution, followed by a second screening by IFA. Hybridoma cells taken from IFA-positive wells that had a single colony per well were cultured and expanded in Hybridoma-SFM (Invitrogen). MAB was purified from 100 ml hybridoma culture supernatant by affinity chromatography using HiTrap Protein G HP Columns (GE Healthcare) and then dialyzed into phosphate buffered saline (PBS) using Slide-A-Lyzer Dialysis Cassettes (Thermo Scientific). Control IgG (D23-1B3B9) used in this study was derived from the PBMCs of a dengue patient infected with dengue virus serotype 2 [33].

Viruses

Eight influenza B vaccine strains (B/Florida/4/2006, B/Malaysia/2506/2004, B/Shanghai/361/2002, B/Johannesburg/5/1999, B/Yamanashi/166/1998, B/Shandong/7/1997, B/Mie/1/1993, and B/Victoria/2/1987) and a mouse-adapted influenza B virus strain (B/Ibaraki/2/1985) were used. The B/Malaysia/2506/2004 and B/Florida/4/2006 strains were kindly provided by the National Institute of Infectious Diseases, Tokyo, Japan. The mouse-adapted B/Ibaraki/2/1985 strain was provided by Dr. S. Tamura, National Institute of Infectious Diseases [44]. Viruses were propagated either in MDCK cells or in 9-day-old embryonated chicken eggs. Infectivity was titrated by focus-forming assay: MDCK cells in a 96-well plate were adsorbed with viruses serially ten-fold diluted at 37°C for 1 hour. The cells were then washed with PBS and incubated at 37°C for 12 hours. Cells were fixed and subjected to IFA.

Characterization of HuMAbs

For IFA, the infected cells were fixed with absolute ethanol for 2 minutes at room temperature and then reacted with hybridoma supernatant for 30 minutes at 37°C, followed by incubation with FITC-conjugated anti-human IgG for 45 minutes at 37°C. For western blotting, the infected samples in a loading buffer containing 2-mercaptoethanol were used for electrophoresis and then blotted to PVDF membrane. They were probed with hybridoma supernatant for 1 hour at 37°C, followed by incubation with HRP-conjugated anti-human IgG for 1 hour at 37°C.

VN assay

The VN test was carried out as described previously [45], with minor modifications. HuMAb at a concentration of 100 µg/ml was serially four-fold diluted with Minimum Essential Medium (MEM; Invitrogen) and incubated with 200 FFU of viruses at 37°C for 1 hour. Then, MDCK cells were adsorbed with the mixtures at 37°C for 1 hour. After incubation for 12 hours, the cells were fixed and subjected to IFA.

HI assay

First, viral titers were determined with a hemagglutination assay. Briefly, the viruses were serially diluted two-fold with PBS and mixed with 0.7% (v/v) human O-type red blood cells. After incubation at room temperature for 1 hour, hemagglutination units (HAUs) were estimated. Next, HI titration was performed as follows: MAb at a concentration of 100 µg/ml was serially two-fold diluted and mixed with 8 HAU per 50 µl of viral sample. After incubation at 37°C for 1 hour, the mixtures were further incubated with 0.7% (v/v) human red blood cells for 1 hour at room temperature. The lowest concentration of HuMAb that completely inhibited hemagglutination was designated the HI titer.

Fusion inhibition assay

Cell-cell fusion was accomplished as described previously [35]. Briefly, monkey kidney cell line CV-1 cells were infected with B/Florida/4/2006 at an MOI of 0.3. After incubation for 24 hours, the cells were washed with MEM and then incubated for 15 minutes at 37°C in MEM supplemented with 2.5 µg/ml of acetylated trypsin (Sigma). After washing, the cells were incubated for 30 minutes with diluted HuMAbs. Thereafter, the cells were treated for 2 minutes at 37°C with MEM supplemented with 10 mM MES and 10 mM HEPES (pH 5.5). After the medium was completely removed by washing, the cells were incubated for 3 hours. Then they were fixed with absolute methanol and stained with Giemsa (Wako).

Surface plasmon resonance analysis (binding kinetics analysis)

Surface plasmon resonance analysis was performed [46] with a Biacore T200 (GE Healthcare). Interaction was measured in running buffer (10 mM HEPES-Na pH 7.5, 150 mM NaCl, 3 mM EDTA, 0.005% Tween 20) at 25°C. The surface of a CM5 sensor chip was coated with goat anti-human IgG Fcγ antibody (Jackson ImmunoResearch) at a density of 10,000 resonance units (RU) by an amine coupling technique using 1-ethyl-3-[3-dimethylaminopropyl] carbodiimide hydrochloride and Sulfo-NHS for activation, and ethanolamine for blocking. As the ligand, each of the anti-HA HuMAbs was captured on the chip surface via anti-human IgG Fcγ to a density of 10–80 RU. The HA protein of B/Florida/4/2006 vaccine antigen (The Research Foundation for Microbial Diseases of Osaka University) was diluted in running buffer at concentrations of 12.5, 25, 50, 100 and 200 nM (as

monomers). Each concentration was injected sequentially on to the chip at a flow rate of 60 µl/min for a contact time of 60 seconds, and then washed with the running buffer for a dissociation time of 30 minutes. Regeneration of the chip surface was performed with 10 mM glycine-HCl pH 1.5. Binding kinetics were evaluated using Biacore T200 evaluation software version 1.0 (GE healthcare) using the single kinetics analysis method with a 1:1 binding model.

Selection of escape mutants

Escape mutants were selected by culturing B/Florida/4/2006 in the presence of HuMAb as described previously [47], with minor modifications. Viruses (to give final concentrations of 100 to 1,000 FFU/ml) were incubated with HuMAb serially ten-fold diluted (to give final concentrations of 0.0025, 0.025, 0.25 and 2.5 µg/ml), at 37°C for 1 hour. Then, MDCK cells in a 24-well plate were inoculated with the mixtures (n=6 for each) and cultured in DMEM/F-12+GlutaMAX-I supplemented with 0.4% bovine serum albumin (BSA), antibiotics and 2 µg/ml acetylated trypsin. After culturing for 72 hours, the supernatants in each well were collected separately and subjected to VN and HI assays. The entire HA gene was directly sequenced from the mixed population in the supernatants of those viral samples that showed a reduced neutralization and HI titer of more than four-fold.

Direct sequencing analysis

Viral RNA extracted with QIAamp Viral RNA Mini Kit (Qiagen) was subjected to one step RT-PCR (Superscript III One-Step RT-PCR System with Platinum *Taq* High Fidelity; Invitrogen) with the following HA primer set: 5'-CAGAATTCAT-GAAGGCAATAATTGTACTAC-3' forward and 5'-CTCfC-GCGGCCGCTTATAGACAGATGGAGCATGAAACG-3' reverse. The PCR products were purified with Qiaquick PCR Purification Kit (Qiagen). After electrophoresis, the discrete band was extracted using the Qiaquick Gel Extraction Kit (Qiagen) and sequenced.

Construction of HA plasmids

HA gene of B/Florida/4/2006 and B/Shanghai/361/2002 was amplified by one step RT-PCR, as described above, and inserted into the pGEM-T Easy Vector (Promega). Mutant and truncated HA genes were generated by site-directed mutagenic PCR (GeneTailor Site-Directed Mutagenesis System; Invitrogen) and conventional PCR (Expand High Fidelity^{PLUS} PCR System; Roche), respectively, using the HA plasmid inserted into pGEM-T easy vector. Each of the plasmids was subcloned into the expression vector pCAGGS/MCSII [48]. The expression plasmids were transfected into human embryonic kidney 293T cells with lipofectamine 2000 (Invitrogen) according to the manufacturer's instructions.

Homology of amino acid sequence

Amino acid sequence and sequence information were downloaded from the FTP site of Influenza Virus Resource (<ftp://ftp.ncbi.nih.gov/genomes/INFLUENZA/>) on January 31, 2012. HA sequences of influenza B virus were extracted from the database, and then aligned using the MAFFT program [49,50]. The number of variants in the target sequence (IGNCPIWVKT) was counted.

IgG isotyping

ELISA microplates (MaxiSorp; Nunc) were coated overnight at 4°C with goat anti-human IgG (Jackson ImmunoResearch Laboratories) in 0.05 M sodium bicarbonate buffer (pH 8.6).

After washing with PBS including 0.1% Tween-20, the wells were blocked with 0.5% BSA in PBS for 1 hour at 37°C. After washing again, the wells were incubated with hybridoma supernatants or control serum for 2 hours at 37°C. Following further washing, the wells were incubated with HRP-conjugated anti-human IgG1, IgG2, IgG3 or IgG4 (SouthernBiotech) for 1 hour at 37°C. The wells were washed five times followed by incubation with TMB peroxidase substrate (KPL) at room temperature in the dark. After 20 minutes, the reaction was stopped with 2N H₂SO₄ solution. The color development was read at 450 nm in an ELISA Photometer (Biotek ELISA Reader; Biotek). All samples were run in triplicate.

Sequencing of HuMAb variable regions

Total RNA extracted from the hybridoma using an RNeasy Mini Kit (Qiagen) was subjected to RT-PCR using a PrimeScript RT reagent Kit (Takara) with an oligo (dT) primer. The coding region of the H- and L-chains of HuMAb was amplified by PCR with the following primers: 5'-ATGGAGTTTGGGCTGAGC-TGGGTT-3' (H-chain-forward) and 5'-CTCCCGCGGCTTT-GTCTTGGCATT-3' (H-chain-reverse); and 5'-ATGGCCTG-GRYCYCMYTCYWCCTM-3' (L-chain-forward) and 5'-TGG-CAGCTGTAGCTTCTGTGGGACT-3' (L-chain-reverse). PCR products were ligated into pGEM-T Easy Vector (Promega) and their sequences were analyzed using a BigDye Terminator v3.1 Cycle Sequencing Kit and an ABI Prism 3100 Genetic Analyzer (Applied Biosystems). Determined sequences were analyzed and compared to the NCBI database using the IgBlast softwares (<http://www.ncbi.nlm.nih.gov/igblast/>).

Molecular modeling

The HA structure was constructed using Molecular Operating Environment software (Chemical Computing Group Inc.) based on the crystal structure of B/Hong Kong/8/1973 (PDB ID: 2RFU) [51].

Passive transfer experiments

All mice used were 6-week-old female BALB/c mice from Japan SLC Inc. Before infection, mice were anesthetized by intraperitoneal administration of pentobarbital sodium (Somnopenyl; Kyoritsu Seiyaku Corporation). MLD₅₀ was determined by inoculating intranasally with serial 10-fold dilutions of virus and calculating with the Reed-Muench method [52]. For passive transfer experiments, mice were treated with HuMAb at 1, 5, 10 or 15 mg/kg intraperitoneally at 4, 24, 48 or 72 hours post-infection with 25 µl mouse-adapted B/Ibaraki/2/1985 virus at a lethal dose (1.47 × 10³ MLD₅₀/mouse). Mice were weighed daily and sacrificed if they fell to 60% of starting weight. To titrate the viruses in the infected lungs, mouse-adapted B/Ibaraki/2/1985 or B/Florida/4/2006 passaged eight times in mice lungs were infected at 1.47 × 10³ MLD₅₀/mouse or 5.0 × 10³ FFU/mouse, respectively. The lungs were harvested on day 3 and day 6 post-infection and virus titers in lung homogenates were determined by focus-forming assay.

Statistical analyses

Data are expressed as the means ± standard errors of the means (SEM). Statistical analysis was performed by Student's *t* test. A *P* value of <0.05 was considered significant.

Accession numbers

The GenBank (<http://www.ncbi.nlm.nih.gov/GenBank/>) accession numbers for the genes discussed in this paper are as

follows: IgG-V_H in clone 5A7 (AB729122), IgG-V_L in clone 5A7 (AB729123), IgG-V_H in clone 3A2 (AB729120), IgG-V_L in clone 3A2 (AB729121), IgG-V_H in clone 10C4 (AB729124), and IgG-V_L in clone 10C4 (AB729125).

Supporting Information

Figure S1 Cell-cell fusion inhibition assay. CV-1 cells were infected with B/Florida/4/2006 treated with HuMAbs 5A7, 3A2, 10C4 or control IgG at pH 5.5. HuMAbs (100 µg/ml) were serially four-fold diluted. As a control for pH, assay with 5A7 was also performed at pH 7.0 (second row). Mock/- (bottom left panel) is a mock-infected sample without HuMAb at pH 5.5. Infection/- (bottom right panel) is an infected sample without HuMAb at pH 5.5, as a positive control. Arrowheads show major cell-cell fusion bodies.

(PDF)

Figure S2 Surface plasmon resonance analysis of binding affinity between HuMAbs and the HA protein of B/Florida/4/2006. HuMAbs 5A7, 3A2 or 10C4 were immobilized on the surface of a CM5 chip via pre-crosslinked anti-human IgG Fcγ antibody. The HA protein at concentrations of 12.5, 25, 50, 100 and 200 nM were consecutively injected onto the chip surface and the association and dissociation phases were monitored. Signal from the chip surface without anti-HA antibody (the reference value) was subtracted from each reading.

(PDF)

Figure S3 Diagram showing how the escape mutants were obtained. Four HuMAb concentrations prepared by serial ten-fold dilutions (right lower diagram) were mixed with B/Florida/4/2006 for 1 hour. Then, each mixture was used to infect MDCK cells in six wells (i.e., four groups of six wells) and incubated for 72 hours (for details, see Materials and methods). Groups were graded according to cytopathic effects: all six wells showing no cytopathic effects (white), some wells showing cytopathic effects (gray), and all wells showing cytopathic effects (black). Supernatants from wells colored gray were collected separately and measured for VN and HI activities. When a four-fold reduction in VN and HI assays was not shown by any of supernatants, one sample was mixed with HuMAbs serially 10-fold diluted described above and infected to newly prepared MDCK cells. P1 to P10 indicates passage number. Out of 12 gray wells, two wells for 3A2 and one well for 10C4 (colored red) showed a four-fold reduction in VN and HI activities compared with the parent virus. Gray wells at P10 of 5A7 and gray and red wells at P1 of 3A2 and 10C4 were subjected to direct sequencing analysis of the HA gene.

(PDF)

Figure S4 The epitope region of 3A2 and 10C4. Escape mutants were selected by incubation of B/Florida/4/2006 with HuMAbs. Amino acid sequences of the HA protein in the escape mutants were compared with the original B/Florida/4/2006. Asterisks indicate amino acid residues that differed between the original virus and the escape mutants.

(PDF)

Figure S5 The additional epitope region of 3A2. Expression plasmids bearing chimeric HA protein were prepared from B/Shanghai/361/2002 (Sh/02) and B/Florida/4/2006 (Flo/06). 293T cells expressing the chimeric protein were subjected to IFA with 3A2 (left panels). White bars represent the amino acid sequence in Sh/02, and black bars represent the amino acid sequence in Flo/06. The different amino acid residues in the HA

protein from each of the two viral strains are shown in the top and bottom bars.

(PDF)

Table S1 Pattern of reactivity of HuMAbs.

(PDF)

Table S2 Homology of the epitope region of HuMAb 5A7 among the corresponding sequences derived from NCBI database.

(PDF)

Acknowledgments

We thank Dr. Shin-ichi Tamura (the National Institute of Infectious Diseases) for providing viral strains. We also thank Ms. Natsuko Fukura,

References

- Lambert LC, Fauci AS (2010) Influenza vaccines for the future. *N Engl J Med* 363: 2036–2044.
- WHO (2009) Influenza (Seasonal). Available: <http://www.who.int/mediacentre/factsheets/fs211/en/>.
- Carrat F, Flahault A (2007) Influenza vaccine: the challenge of antigenic drift. *Vaccine* 25: 6852–6862.
- Nobusawa E, Sato K (2006) Comparison of the mutation rates of human influenza A and B viruses. *J Virol* 80: 3675–3678.
- Webster RG, Berton MT (1981) Analysis of antigenic drift in the haemagglutinin molecule of influenza B virus with monoclonal antibodies. *J Gen Virol* 54: 243–251.
- Hay AJ, Gregory V, Douglas AR, Lin YP (2001) The evolution of human influenza viruses. *Philos Trans R Soc Lond B Biol Sci* 356: 1861–1870.
- Lin YP, Gregory V, Bennett M, Hay A (2004) Recent changes among human influenza viruses. *Virus Res* 103: 47–52.
- Sym D, Patel PN, El-Chaar GM (2009) Seasonal, avian, and novel H1N1 influenza: prevention and treatment modalities. *Ann Pharmacother* 43: 2001–2011.
- Belshe RB (2010) The need for quadrivalent vaccine against seasonal influenza. *Vaccine* 28 Suppl 4: D45–53.
- Nicholson KG, Aoki FY, Osterhaus AD, Trotter S, Carewicz O, et al. (2000) Efficacy and safety of oseltamivir in treatment of acute influenza: a randomised controlled trial. *Neuraminidase Inhibitor Flu Treatment Investigator Group. Lancet* 355: 1845–1850.
- Aoki FY, Macleod MD, Paggiaro P, Carewicz O, El Sawy A, et al. (2003) Early administration of oral oseltamivir increases the benefits of influenza treatment. *J Antimicrob Chemother* 51: 123–129.
- Kiso M, Mitamura K, Sakai-Tagawa Y, Shiraiishi K, Kawakami C, et al. (2004) Resistant influenza A viruses in children treated with oseltamivir: descriptive study. *Lancet* 364: 759–765.
- Lowen AC, Palese P (2007) Influenza virus transmission: basic science and implications for the use of antiviral drugs during a pandemic. *Infect Disord Drug Targets* 7: 318–328.
- Reece PA (2007) Neuraminidase inhibitor resistance in influenza viruses. *J Med Virol* 79: 1577–1586.
- Suzuki Y, Taira K, Saito R, Nidaira M, Okano S, et al. (2009) Epidemiologic study of influenza infection in Okinawa, Japan, from 2001 to 2007: changing patterns of seasonality and prevalence of amantadine-resistant influenza A virus. *J Clin Microbiol* 47: 623–629.
- Jing X, Ma C, Ohigashi Y, Oliveira FA, Jardtzyk TS, et al. (2008) Functional studies indicate amantadine binds to the pore of the influenza A virus M2 proton-selective ion channel. *Proc Natl Acad Sci U S A* 105: 10967–10972.
- Marasco WA, Sui J (2007) The growth and potential of human antiviral monoclonal antibody therapeutics. *Nat Biotechnol* 25: 1421–1434.
- Campas-Moya C (2010) Golimumab: A novel anti-TNF-alpha human monoclonal antibody for rheumatoid arthritis, psoriatic arthritis and ankylosing spondylitis. *Drugs Today (Barc)* 46: 13–22.
- Cheson BD (2010) Ofatumumab, a novel anti-CD20 monoclonal antibody for the treatment of B-cell malignancies. *J Clin Oncol* 28: 3525–3530.
- Shirahata S, Katakura Y, Teruya K (1998) Cell hybridization, hybridomas, and human hybridomas. *Methods Cell Biol* 57: 111–145.
- Lonberg N (2005) Human antibodies from transgenic animals. *Nat Biotechnol* 23: 1117–1125.
- Clackson T, Hoogenboom HR, Griffiths AD, Winter G (1991) Making antibody fragments using phage display libraries. *Nature* 352: 624–628.
- McCafferty J, Griffiths AD, Winter G, Chiswell DJ (1990) Phage antibodies: filamentous phage displaying antibody variable domains. *Nature* 348: 552–554.
- Jin A, Ozawa T, Tajiri K, Obata T, Kondo S, et al. (2009) A rapid and efficient single-cell manipulation method for screening antigen-specific antibody-secreting cells from human peripheral blood. *Nat Med* 15: 1088–1092.
- Nelson AL, Dhimolea E, Reichert JM (2010) Development trends for human monoclonal antibody therapeutics. *Nat Rev Drug Discov* 9: 767–774.
- Ekiert DC, Bhabha G, Elsigler MA, Friesen RH, Jongeneelen M, et al. (2009) Antibody recognition of a highly conserved influenza virus epitope. *Science* 324: 246–251.
- Sui J, Hwang WC, Perez S, Wei G, Aird D, et al. (2009) Structural and functional bases for broad-spectrum neutralization of avian and human influenza A viruses. *Nat Struct Mol Biol* 16: 265–273.
- Ekiert DC, Friesen RH, Bhabha G, Kwaks T, Jongeneelen M, et al. (2011) A highly conserved neutralizing epitope on group 2 influenza A viruses. *Science* 333: 843–850.
- Corti D, Voss J, Gamblin SJ, Codoni G, Macagno A, et al. (2011) A neutralizing antibody selected from plasma cells that binds to group 1 and group 2 influenza A hemagglutinins. *Science* 333: 850–856.
- Dreyfus C, Laursen NS, Kwaks T, Zuijdgheest D, Khayat R, et al. (2012) Highly conserved protective epitopes on influenza B viruses. *Science* 337: 1343–1348.
- Kubota-Koketsu R, Mizuta H, Oshita M, Ideno S, Yunoki M, et al. (2009) Broad neutralizing human monoclonal antibodies against influenza virus from vaccinated healthy donors. *Biochem Biophys Res Commun* 387: 180–185.
- MBL (2010) Press release (Generation of fully human monoclonal antibodies neutralizing influenza virus). Available: <http://www.mbl.co.jp/e/ir/2010/0112.html>.
- Setthapramote C, Sasaki T, Puiprom O, Limkittikul K, Pitaksajjakul P, et al. (2012) Human monoclonal antibodies to neutralize all dengue virus serotypes using lymphocytes from patients at acute phase of the secondary infection. *Biochem Biophys Res Commun* 423: 867–872.
- Wang Q, Cheng F, Lu M, Tian X, Ma J (2008) Crystal structure of unliganded influenza B virus hemagglutinin. *J Virol* 82: 3011–3020.
- Okuno Y, Isegawa Y, Sasao F, Ueda S (1993) A common neutralizing epitope conserved between the hemagglutinins of influenza A virus H1 and H2 strains. *J Virol* 67: 2552–2558.
- Okuno Y, Matsumoto K, Isegawa Y, Ueda S (1994) Protection against the mouse-adapted A/FM/1/47 strain of influenza A virus in mice by a monoclonal antibody with cross-neutralizing activity among H1 and H2 strains. *J Virol* 68: 517–520.
- Knossow M, Gaudier M, Douglas A, Barrere B, Bizebard T, et al. (2002) Mechanism of neutralization of influenza virus infectivity by antibodies. *Virology* 302: 294–298.
- Wang TT, Tan GS, Hai R, Pica N, Petersen E, et al. (2010) Broadly protective monoclonal antibodies against H3 influenza viruses following sequential immunization with different hemagglutinins. *PLoS Pathog* 6: e1000796.
- Yoshida R, Igarashi M, Ozaki H, Kishida N, Tomabechi D, et al. (2009) Cross-protective potential of a novel monoclonal antibody directed against antigenic site B of the hemagglutinin of influenza A viruses. *PLoS Pathog* 5: e1000350.
- Chakrabarti BK, Walker LM, Guenaga JF, Ghobbeh A, Poignard P, et al. (2011) Direct antibody access to the HIV-1 membrane-proximal external region positively correlates with neutralization sensitivity. *J Virol* 85: 8217–8226.
- Casipit CL, Tal R, Wittman V, Chavallaz PA, Arbuthnot K, et al. (1998) Improving the binding affinity of an antibody using molecular modeling and site-directed mutagenesis. *Protein Sci* 7: 1671–1680.
- Chames P, Coulon S, Baty D (1998) Improving the affinity and the fine specificity of an anti-cortisol antibody by parsimonious mutagenesis and phage display. *J Immunol* 161: 5421–5429.
- Petukhova G, Naikhin A, Chirkova T, Domina S, Korenkov D, et al. (2009) Comparative studies of local antibody and cellular immune responses to influenza infection and vaccination with live attenuated reassortant influenza vaccine (LAIV) utilizing a mouse nasal-associated lymphoid tissue (NALT) separation method. *Vaccine* 27: 2580–2587.
- Chen Z, Kadowaki S, Hagiwara Y, Yoshikawa T, Sata T, et al. (2001) Protection against influenza B virus infection by immunization with DNA vaccines. *Vaccine* 19: 1446–1455.
- Okuno Y, Tanaka K, Baba K, Maeda A, Kunita N, et al. (1990) Rapid focus reduction neutralization test of influenza A and B viruses in microtiter system. *J Clin Microbiol* 28: 1308–1313.

Dr. Azusa Asai and Dr. Yohei Watanabe for their helpful advice and technical assistance; Dr. Pratap Singhasivanon for his continuous encouragement and valuable discussion about this project; and Dr. Pathom Sawanpanyalert and Dr. Jotika Boon-Long for the coordination of the JST/JICA, SATREPS projects.

Author Contributions

Conceived and designed the experiments: MY KI. Performed the experiments: MY RKK AD TS MN RM NB. Analyzed the data: MY AY NK KF YO TN KI. Contributed reagents/materials/analysis tools: MK. Wrote the paper: MY KI. Performed the molecular modeling: NK.

46. Chen C, Wang S, Wang H, Mao X, Zhang T, et al. (2012) Potent neutralization of botulinum neurotoxin/b by synergistic action of antibodies recognizing protein and ganglioside receptor binding domain. *PLoS One* 7: e43845.
47. Gulati U, Hwang CC, Venkatramani L, Gulati S, Stray SJ, et al. (2002) Antibody epitopes on the neuraminidase of a recent H3N2 influenza virus (A/Memphis/31/98). *J Virol* 76: 12274–12280.
48. Ueda M, Daidoji T, Du A, Yang CS, Ibrahim MS, et al. (2010) Highly pathogenic H5N1 avian influenza virus induces extracellular Ca²⁺ influx, leading to apoptosis in avian cells. *J Virol* 84: 3068–3078.
49. Katoh K, Misawa K, Kuma K, Miyata T (2002) MAFFT: a novel method for rapid multiple sequence alignment based on fast Fourier transform. *Nucleic Acids Res* 30: 3059–3066.
50. Katoh K, Toh H (2008) Recent developments in the MAFFT multiple sequence alignment program. *Brief Bioinform* 9: 286–298.
51. Wang Q, Tian X, Chen X, Ma J (2007) Structural basis for receptor specificity of influenza B virus hemagglutinin. *Proc Natl Acad Sci U S A* 104: 16874–16879.
52. Ozanne G (1984) Estimation of endpoints in biological systems. *Comput Biol Med* 14: 377–384.

Evolution and control of H5N1

A better understanding of the evolution and diversity of H5N1 flu virus and its host species in endemic areas could inform more efficient vaccination and control strategies

Yohei Watanabe, Madiha S. Ibrahim & Kazuyoshi Ikuta

The H5N1 virus has spread across Asia, Europe and Africa, and has infected birds in several endemic areas, including China, Indonesia, Vietnam and Egypt. H5N1 outbreaks pose a massive threat for the poultry industry and, ultimately, for human health [1]. However, the rapid spread of the virus also offers the opportunity to study and learn from its dynamics in the wild. The insights gained should inform new public health policies and preventive actions against a possible pandemic.

Progress in influenza research has been impressive. In particular, the application of reverse genetics has led to the identification of mutations and reassortment changes that determine virus virulence. Perhaps the most significant results come from the two now infamous studies, published in *Nature* and *Science*, about the generation of recombinant H5N1 viruses that are transmissible in ferrets [2,3]. These advances show that we are steadily elucidating influenza virus at the molecular level. By contrast, our understanding of the dynamics of highly pathogenic influenza virus in the environment remains limited [4,5].

Highly pathogenic avian influenza (HPAI) is an important poultry disease. The major reservoir of the virus is wild waterfowl, and infected birds are usually asymptomatic as a result of long-term evolutionary adaptation [1,6]. After transmission from wild waterfowl to poultry, however, avian influenza viruses occasionally become highly pathogenic and can cause mortalities of up to 100% within 48 h of infection. The standard method for controlling an HPAI outbreak is the testing and culling of all infected poultry, and the setting up of a concentric control area around the infected flock.

The HPAI H5N1 virus, circulating in Eurasia and Africa, emerged in China around 1997 [1] but it only infected terrestrial birds at the time. Continuous transmission in poultry eventually allowed the virus to evolve, resulting in large outbreaks in China in 2005 with high mortality in wild waterfowl. The virus spread rapidly, probably through migratory birds, to Central Asia, Europe, the Middle East and Africa. Such 'east to west' movements of H5N1 viruses over comparably long distances have not since been recorded. Moreover, migrating wildfowl have begun to spread the virus intermittently between Asia and Siberia [7]. This H5N1 lineage is the longest-circulating HPAI virus that has been reported, and it has reached epizootic levels in both domestic and wild bird populations.

...the challenge is to understand the evolution of H5N1 to better predict new strains that could become a serious threat for human health

One of the striking characteristics of the H5N1 lineage, in contrast with other HPAI, is its infectivity toward mammals. H5N1 can be directly transmitted from birds to humans and cause severe disease, although it has a significantly lower transmissibility than seasonal influenza viruses [1]. So far, 608 cases of human H5N1 infections have been reported with 59% mortality [5]. Most human infections have resulted from close contact with H5N1-infected poultry or poultry products, and no sustained human-human transmission has as yet been documented.

...continuous replication of H5N1 virus in Egypt has provided a valuable opportunity to study the impact of genetic evolution on phenotypic variation without reassortment

Nonetheless, a potential H5N1 pandemic remains a great concern for public health.

The viruses that caused the five influenza pandemics since 1900 arose by two mechanisms: reassortment among avian, human and swine influenza viruses, and accumulation of mutations in an avian influenza virus [1,8]. Triple reassortment between avian H5N1, swine H3N1 and H1N1 viruses, and double reassortment between avian H5N1 and H9N2 viruses has already been reported in Asia, which raises concerns about new reassortment viruses that could infect humans [9,10]. Meanwhile, research has identified some 80 genetic mutations that could increase infectivity of avian influenza viruses in mammals, and thus potentially facilitate avian influenza evolution to generate a pandemic strain [8,11]. H5N1 strains with some of these mutations have often been found in bird populations [5] and in human H5N1 strains [12]. Indeed, specific mutations that could confer switching in receptor-binding specificity were reported in H5N1-infected patients in Thailand [13]. The two controversial studies published in *Nature* and *Science* also showed how a handful of mutations might enable the H5N1 virus to be transmitted between humans [2,3]. Pathogenic variants of the H5N1 virus with a higher pandemic potential could naturally evolve; the challenge is to understand the evolution of H5N1 to better predict new strains that could become a serious threat for human health.

The evolutionary dynamics of the Egyptian H5N1 strains provide clues to understanding the pandemic potential of H5N1. The virus was introduced only once in Egypt, in early 2006, and spread among a variety of bird species, including chickens, ducks, turkeys, geese and quail [14]. The virus rapidly evolved to form a phylogenetically distinct clade that has since diverged into multiple sublineages [15]. Thus, continuous replication of H5N1 virus in Egypt has provided a valuable opportunity to study the impact of genetic evolution on phenotypic variation without reassortment.

After diversification in local bird populations, some new H5 sublineages have emerged in Egypt with a higher affinity for human-type receptors. Indeed, since their emergence in 2008, almost all human H5N1 strains in Egypt have been phylogenetically grouped into these new sublineages, which can be transmitted to humans with a higher efficacy than other avian influenza viruses. This might explain why, since 2009, Egypt has had the highest number of human cases of H5N1 infection, with more than 50% of the cases worldwide [5]. Fortunately, these Egyptian H5N1 sublineages still do not have binding affinity for receptors in the upper respiratory tract and, therefore, do not sustain transmission in humans. However, it increases the risk of H5N1 variants that are better adapted to humans after viral replication in infected patients.

...Egypt is regarded as the country with the highest H5N1 pandemic potential worldwide

The Egyptian H5N1 sublineages are also diversifying antigenically in the field, as some are no longer crossreactive to other co-circulating sublineages [15]. Moreover, faint traces of species-specific evolutionary changes have been detected [16], implying a change in their host species. It shows that the H5N1 virus has undergone significant diversification in Egypt during the past seven years. Of greater concern, however, are Egyptian H5N1 strains that carry mammalian influenza virus type PB2 and have lost the N-linked 158 glycosylation site in the top region of haemagglutinin [15,17], both of which can potentially facilitate viral transmission to humans. The genetic diversification of H5N1 virus in Egypt represents an increasing pandemic

potential, and Egypt is regarded as the country with the highest H5N1 pandemic potential worldwide [18].

A similar situation exists in other geographical areas. Multiple clades and sublineages of H5N1 are co-circulating in Asia, occasionally enabling reassortment events within and beyond the viral subtypes in the field [19,20]. Several H5N1 strains with enhanced binding affinity to human-type receptors have been reported in Indonesia [12]. Similarly, avian and swine H5N1 strains with an altered receptor-binding preference have been isolated sporadically in Indonesia and Laos [21,22]. As in other areas, distinct groups of H5N1 viruses are circulating amongst themselves and with other avian influenza viruses, generating diverse viral phenotypes in nature. The evolutionary dynamics of H5N1 might even accelerate in the wild. H5N1 viruses diverge genetically in ducks [23]; they can transfer the virus over long distances by migration. Thus, the H5N1 virus has established a complex life cycle in nature with accelerated evolutionary dynamics. The pandemic threat of H5N1 remains a serious concern and might be increasing.

Control measures based on isolating and culling are still the gold standard for controlling the early phase of an H5N1 outbreak, and worked against the H5N1 outbreaks in Hong Kong in 1997 and in Thailand in 2004 [4]. However, this measure failed in several countries and made H5N1 endemic. Cross-border circulation of H5N1 further complicates implementation of a classical control strategy based on culling in the infected area.

In response, public health officials in several countries, including Egypt and Indonesia, advocate poultry vaccination as a preventive or adjunct control measure [1]. Although vaccination does not completely prevent infections, its proper use can help to control avian influenza outbreaks by reducing virus transmission from infected animals. However, it can also increase vaccine-driven evolution among avian influenza viruses. The endemic status of H5N1, which can cause devastating local epidemics, puts pressure on health officers to use a vaccine or a vaccination strategy that might eventually increase selective pressure and thereby accelerate H5N1 evolution. Given the high mutability and diversity of circulating viruses, it seems best

to avoid using a vaccine based on a strain from a different geographical area because there would only be a partial antigen match; such a heterologous vaccine would only be effective in the short term compared with a homologous vaccine. During past control of H5N1 epidemics using imported vaccines, escape mutants have emerged within about a year of the start of vaccination, which made the epidemic even worse [14]. When a vaccination strategy is implemented in an endemic area, the vaccine seed strain should be selected from the same geographical area to try to get the longest possible protection. Vaccine seed virus selection must be periodically revised to produce well-matched and efficacious vaccines.

Close communication and workshops hold the greatest potential for controlling the H5N1 virus

In most cases, H5 vaccine for an endemic area comes from a foreign supplier. It would be necessary to enable foreign manufacturers to produce customized H5 vaccines based on epidemic strains from different areas. The best approach might be a plasmid-based reverse genetics system to construct vaccine seed viruses [1]. In egg-based production, which is the basis of flu vaccine production, the seed virus needs to be adapted for high growth. This time-consuming step carries the risk of antigenic changes during vaccine production. Yet, advances in influenza reverse genetics have led to the development of cell culture systems to produce recombinant viruses, which would enable rapid genetic mutagenesis and reassortment. Once reverse genetics generates a virus genome that is well adapted to growth in cell culture, the haemagglutinin and neuraminidase genes can be easily interchanged with those of other influenza viruses. In addition, virus growth in cell culture can shorten production time, which increases the probability of selecting a seed virus antigenically appropriate for the upcoming flu season, and enables a rapid increase in production if necessary [24].

A control strategy imposed without consideration of regional customs will not be successful

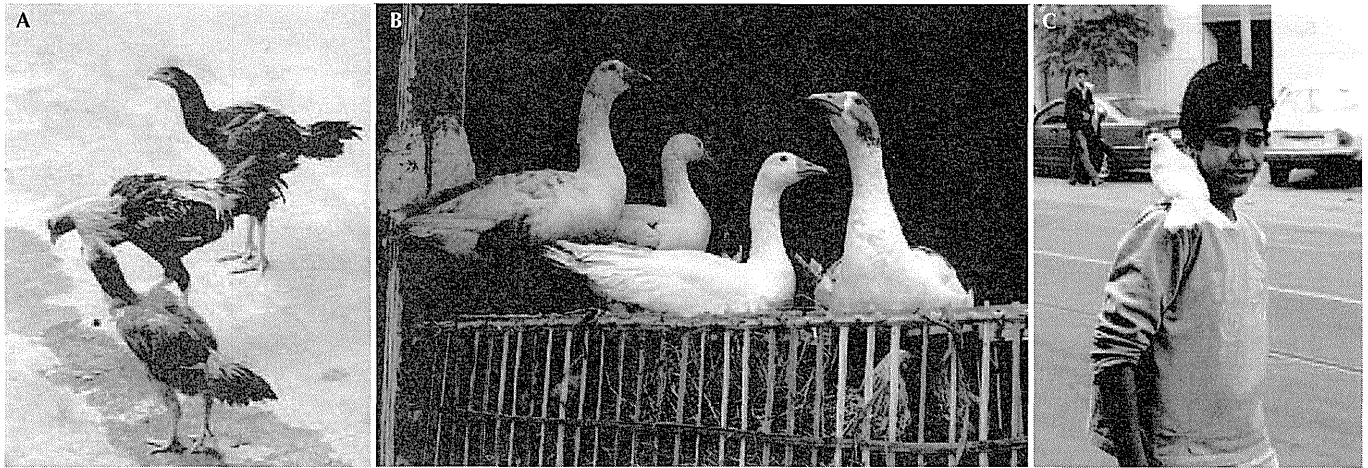


Fig 1 | Socio-cultural traditions in rearing birds for food in Egypt. (A) Free rearing of backyard birds. (B) Live birds at a downtown market. (C) An example of the intertwined relationship between birds and humans.

Given the zoonotic risks of influenza viruses to both humans and animals, the establishment of a vaccine production system applicable to both human and animal infections is an urgent issue. The capacity of vaccine production needs to be flexible for seasonal, pre-pandemic and pandemic vaccines. Advances in genetic engineering facilitate *in vitro* control of human- and avian-type receptor expression on cultured cells, which should allow both human and avian influenza viruses to grow in the same system. As vaccine production capacity based on cell culture develops, commercial production of H5N1 vaccines tailored to each geographical area should become possible. In addition, emergency vaccination guidelines, such as pre-pandemic vaccine stockpiling, expanding and accelerating vaccine production and setting vaccination priorities, should be formulated in a business–government partnership, to ensure pandemic preparation. There is no guarantee that the H5N1 virus will be the next pandemic influenza strain. However, exploring options for versatile vaccine manufacturing is a key to controlling zoonotic influenza viruses, including H5N1.

The complexity of H5N1 ecology also makes control of endemic H5N1 by vaccination a complex task. The problem is that antigenically different groups of viruses, which are not crossreactive, are often co-circulating in endemic areas. Circulation of viruses in each sublineage is not restricted in terms of geography or host species, which complicates efforts to use a vaccine produced against antigens from

a single virus strain [15]. Of greater concern, H5N1 virus infects a variety of bird species [1], which means the vaccination targets have expanded. Bird species differ in their optimal vaccination protocol—for example, the single vaccination used routinely in chickens does not induce an adequate immune response in turkeys, which require multi-dose vaccination at an older age [25]. Furthermore, rearing many bird species and their hybrid breeds in uncontrolled confinement is common in H5N1 endemic countries, especially in rural areas. Therefore, the immunogenicity of existing vaccines is probably inadequate to protect all target species with a single vaccination scheme. Endemic H5N1 already forces public health officials to redefine vaccine development policy to improve both vaccine immunogenicity and vaccination regime.

Unfortunately, it is unlikely that science will ever produce a clear answer as to when, where and how the next pandemic influenza virus will emerge

Today, there are numerous techniques that could overcome these problems by increasing immunogenic potency and crossreactivity. Innovative vaccine formats—multivalent, universal, nasal and synthetic vaccines—possibly coupled with the use of adjuvants, could improve the global vaccine supply [24]. These new technologies should be applied as soon as

possible. Nevertheless, no single technique can probably resolve the underlying complexity of H5N1 dynamics. Over-reliance on vaccination might therefore only worsen the situation. Vaccination can help control endemic H5N1 only when administered as part of an integrated control programme that includes surveillance, culling, restricting host movement and enhanced quarantine and biosecurity.

The complex evolutionary dynamics of the H5N1 virus are challenging host species barriers and the ecology brings H5N1 into close proximity to humans [1]. The close link between the virus and humans is a multifaceted phenomenon that can affect health in myriad ways. Thus, we need to redefine control strategies to address the nature of H5N1 dynamics. Surveillance is the basis of infection control in the field. Wild birds and their predators should be included as surveillance targets, thereby expanding the H5N1 host species range. Another drawback is the fact that epidemiological studies focus mainly on virus genotyping. Although genetic data is informative, the diversity of H5N1 viruses makes characterization based only on genetic traits difficult. Characterization of viral phenotypes—antigenicity, receptor-binding preference, pathogenicity and transmissibility—is equally important for investigating the evolutionary dynamics of H5N1 viruses in nature. We would need techniques to determine easily viral phenotype, in particular new rapid diagnostic systems that can be used for timely epidemiological

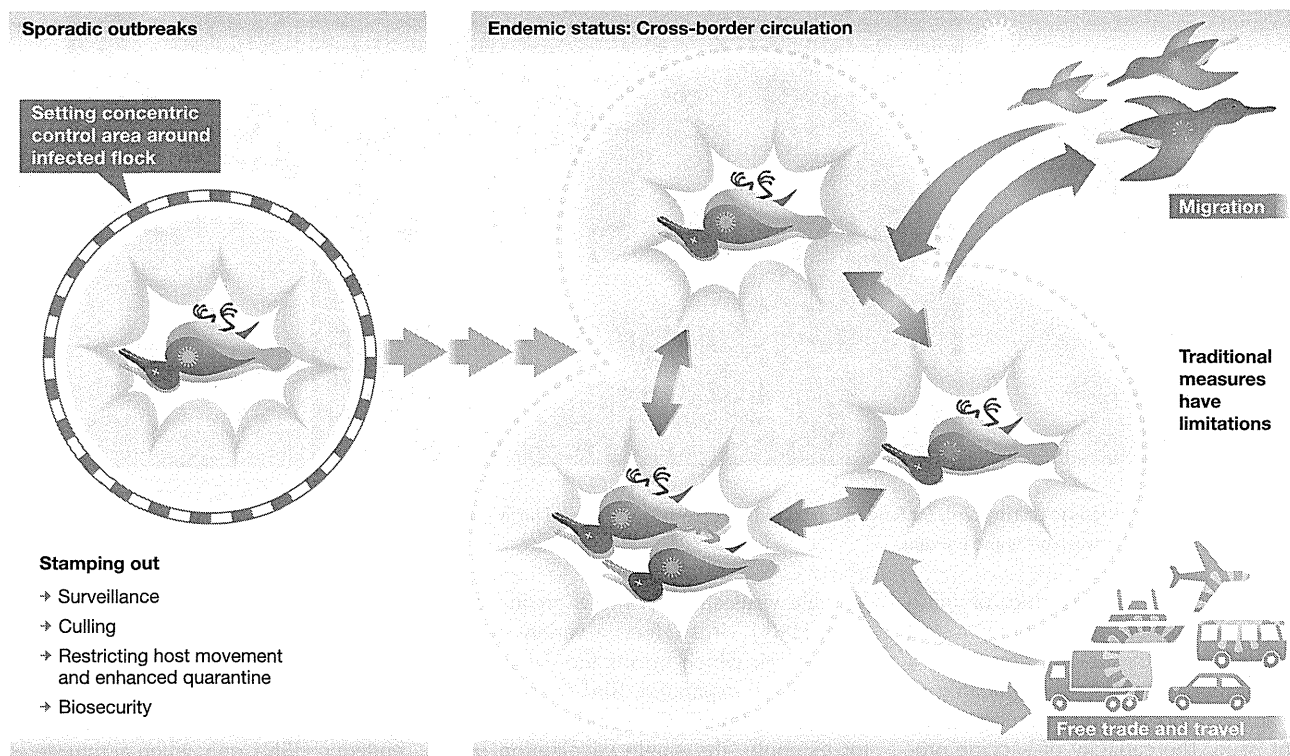


Fig 2 | Changing dynamics of H5N1 virus in the field. Endemic H5N1 virus diversifies in nature, making traditional control measures extremely difficult.

investigations and rapid infection control measures [1]. For example, portable kits that can determine virus receptor specificity would allow field testing of whether a particular avian influenza virus strain has adapted to human-type receptors, thereby adding a new dimension for characterizing and assessing H5N1 outbreaks.

Our perception of H5N1 control should change from short-term hunting to long-term control

The large-scale slaughter of all known and suspected infected birds in H5N1 endemic countries is hugely expensive in terms of execution costs and compensation for lost poultry. Financial assistance from international organizations might be needed to promote the thorough implementation of such a policy. However, H5N1 endemic countries are not all poor nations and some have already built a certain level of technology infrastructure. Thus, transfer of epidemiological skills and concepts to local health officers and scientists is a priority. Overseas collaborations between technologically developed

countries and their institutions, and H5N1 endemic countries and their institutions, should be established at a functional level. Close communication and workshops hold the greatest potential for controlling the H5N1 virus. Such projects supported by governments and funding agencies would encourage establishment of bilateral and multilateral relationships between developed countries and the developing countries, which are the epicentres of H5N1 outbreaks. Sharing information about risk and risk management is one of the key methods for reducing the threat of future H5N1 epidemics.

Globalization has had major benefits for international travel and trade, and sharing of information. The improvements in information technology have dramatically increased the speed and ease of data flow [26]. Intelligence networks facilitate instantaneous sharing of information and enable global warnings about potential hazards as well as problem-solving. Moreover, collaborative research centres, which have been established on reciprocal bases between scientifically advanced countries and institutes and overseas partner countries and institutes in Asia, Africa

and Latin America, are important players in information networking—for instance the Institute Pasteur Network, the Mahidol Oxford Tropical Medicine Research Unit and Japan Initiative for Global Research Network on Infectious Diseases. Linking such laboratory-based networks should be the next step. This would have a profound synergistic effect by maximizing research capacity, human resources and geographic coverage to build a robust global-scale network for infection control.

However, regional socio-cultural issues can be a significant concern for virus control wherever accepted values and scientific understanding might differ. Multiple local and regional factors—customs, religion, politics and economics—can affect H5N1 control in an area. Successful implementation of an H5N1 control strategy depends largely on mutual understanding and consideration of local idiosyncrasies.

Some examples from Egypt show how regional identity can be closely linked with local public health initiatives. Egypt is an Islamic nation and bird meat is an important source of animal protein, and the only

source in some rural areas [14]. A large proportion of Egyptian households in rural areas raise poultry. Although broiler and layer chickens are raised under modern hygienic controls on commercial farms, backyard birds are raised in open uncontrolled farms, leaving them free to interact with other birds (Fig 1A). The poultry meat trade depends mainly on live bird markets in traditional bazaars (Fig 1B), because of a preference for freshly slaughtered poultry. Pigeon towers are built on farms, backyards and roofs throughout villages to raise pigeons for eating. Generally, birds in Egypt are raised in proximity to humans (Fig 1C), which presents an increasing risk of human H5N1 infection in Egypt and establishment of endemic H5N1 in birds nationwide.

Such regional identity is inseparable from socio-cultural contexts, making fundamental change virtually impossible. Although there are many scenarios in which a local public health system could be improved by food safety standards and veterinary inspection or short-term closing of live bird markets for virus clearance, H5N1 control measures have to be implemented whilst respecting the intrinsic socio-cultural traditions in the region. A control strategy imposed without consideration of regional customs will not be successful. It is the local health officers and scientists who are best suited to address the enormous complexity and breadth of issues required for H5N1 control. They also experience H5N1 outbreaks in their area on a regular basis and have a great incentive to be involved in infection control. Therefore, it is important to include local expertise in planning and implementing a control strategy.

Science is frequently looked at as if it can produce a 'silver bullet' to solve every problem. Early success in vaccine and antibiotic development also created a false sense of optimism that scientific methods could eliminate the risk of infection. However, the reality has turned out to be different—some infectious diseases remain uncontrollable and far from eradication. Given the mutable and diversifying nature of avian influenza viruses, there is a significant possibility that different avian influenza subtypes and strains do not follow a single evolutionary pathway. Unfortunately, it is unlikely that science will ever produce a clear answer as to when, where and how the next pandemic influenza virus will emerge. Our

perception of H5N1 control should change from short-term hunting to long-term control. The ecology of H5N1 virus brings it into close proximity to humans. The most important strategy is to minimize contact between terrestrial poultry and wild waterfowl to segregate H5N1 in poultry, because H5N1 spread would be uncontrollable if it established a stable equilibrium in waterfowl. For example, H5N1 viruses in Siberia have not been consistently isolated each year from carcasses and faeces of wildfowl migrating from Asia [7]. This implies that H5N1 circulation in the wild still largely depends on occasional introduction from poultry. It is possible that trials to limit H5N1 infection in poultry would lead to a reduction in viral spread and a dwindling evolutionary path in nature. Infection control policy must abandon fixed strategies in favour of flexible ones to keep pace with the evolutionary dynamics of pathogens such as H5N1 (Fig 2).

Science in an area such as infectious disease research can no longer be viewed as independent of societal needs...

Today's infection control strategy is becoming largely dependent on the reliability and accuracy of information networking. However, the vast flood of scientific information can hide erroneous information and easily mislead the public [26]. Of greater concern, globalization has prompted the centralization of capital and resources, which can lead to an overemphasis on certain research topics. As a consequence, research projects are often short term, without consideration of effects that might have a long-term social impact [27]. This has led to a debate about whether to limit publication of certain types of research or keep scientific information completely accessible. There is probably no easy answer to this. Our global society needs a more mature approach to support research projects that are accurate reflections of societal needs in public health. At the same time, the increasing links between science and society put more pressure on science to play a greater role in society. This is a serious dilemma—how to use science to solve societal problems whilst maintaining its autonomy [27]. Science in an area such as infectious disease research can no longer be viewed as independent

of societal needs; we need to establish a balance between the pursuit of independent basic research and its application for solving clinical problems and crises.

ACKNOWLEDGEMENTS

We thank Y. Suzuki, T. Nakaya, Y. Okuno, K. Takahashi, T. Sasaki, T. Daidoji and R. Kubota-Koketsu for valuable advice and discussions. This work was supported by a Grant-in Aid for Scientific from the Ministry of Education, Culture, Sports, Science and Technology, Japan (grant numbers 23791134 and 23406017) and the Japan Society for the Promotion of Science (JPPS) through the 'Bilateral Programs' scheme.

CONFLICT OF INTEREST

The authors declare that they have no conflict of interest.

REFERENCES

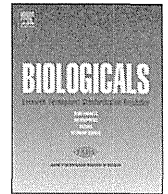
1. Watanabe Y, Ibrahim MS, Suzuki Y, Ikuta K (2012) The changing nature of avian influenza A virus (H5N1). *Trends Microbiol* **20**: 11–20
2. Herfst S *et al* (2012) Airborne transmission of influenza A/H5N1 virus between ferrets. *Science* **336**: 1534–1541
3. Imai M *et al* (2012) Experimental adaptation of an influenza H5 HA confers respiratory droplet 334 transmission to a reassortant H5 HA/H1N1 virus in ferrets. *Nature* **486**: 420–428
4. OIE (2012) Update on highly pathogenic avian influenza in animals (type H5 and H7). <http://www.oie.int/animal-health-in-the-world/update-on-avian-influenza/2012/>
5. WHO (2012) Cumulative number of confirmed human cases of avian influenza A(H5N1) reported 338 to WHO. http://www.who.int/influenza/human_animal_interface/H5N1_cumulative_table_archives/en/index.html
6. Webster RG, Bean WJ, Gorman OT, Chambers TM, Kawaoka Y (1992) Evolution and ecology of influenza A viruses. *Microbiol Rev* **56**: 152–179
7. Sakoda Y *et al* (2010) Characterization of H5N1 highly pathogenic avian influenza virus strains isolated from migratory waterfowl in Mongolia on the way back from the southern Asia to their northern territory. *Virology* **406**: 88–94
8. Medina RA, Garcia-Sastre A (2011) Influenza A viruses: new research developments. *Nat Rev Microbiol* **9**: 590–603
9. Dong G *et al* (2011) Reassortant H9N2 influenza viruses containing H5N1-like PB1 genes isolated from black-billed magpies in Southern China. *PLoS ONE* **6**: e25808
10. Zhou H, Zhang A, Chen H, Jin M (2011) Emergence of novel reassortant H3N2 influenza viruses among ducks in China. *Arch Virol* **156**: 1045–1048
11. Imai M, Kawaoka Y (2012) The role of receptor binding specificity in interspecies transmission of influenza viruses. *Curr Opin Virol* **2**: 160–167
12. Yamada S *et al* (2006) Haemagglutinin mutations responsible for the binding of H5N1 influenza A viruses to human-type receptors. *Nature* **444**: 378–382

13. Kongchanagul A, Suptawiwat O, Kanrai P, Uiprasertkul M, Puthavathana P, Auewarakul P (2008) Positive selection at the receptor-binding site of haemagglutinin H5 in viral sequences derived from human tissues. *J Gen Virol* **89**: 1805–1810
14. Abdelwhab EM, Hafez HM (2011) An overview of the epidemic of highly pathogenic H5N1 avian influenza virus in Egypt: epidemiology and control challenges. *Epidemiol Infect* **139**: 647–657
15. Watanabe Y, Ibrahim MS, Ellakany HF, Kawashita N, Daidoji T, Takagi T, Yasunaga T, Nakaya T, Ikuta K (2012) Antigenic analysis of highly pathogenic avian influenza virus H5N1 sublineages co-circulating in Egypt. *J Gen Virol* **93**: 2215–2226
16. Ibrahim MS, Watanabe Y, Ellakany HF, Yamagishi A, Sapsutthipas S, Toyoda T, Abd El-Hamid HS, Ikuta K (2011) Host-specific genetic variation of highly pathogenic avian influenza viruses (H5N1). *Virus Genes* **42**: 363–368
17. Watanabe Y et al (2011) Acquisition of human-type receptor binding specificity by new H5N1 influenza virus sublineages during their emergence in birds in Egypt. *PLoS Pathog* **7**: e1002068
18. Yong E (2012) Mutant-flu paper published. *Nature* **485**: 13–14
19. Takano R, Nidom CA, Kiso M, Muramoto Y, Yamada S, Sakai-Tagawa Y, Macken C, Kawaoka Y (2009) Phylogenetic characterization of H5N1 avian influenza viruses isolated in Indonesia from 2003–2007. *Virology* **390**: 13–21
20. Nguyen T et al (2012) Evolution of highly pathogenic avian influenza (H5N1) virus populations in Vietnam between 2007 and 2010. *Virology* **432**: 405–416
21. Boltz DA et al (2010) Emergence of H5N1 avian influenza viruses with reduced sensitivity to neuraminidase inhibitors and novel reassortants in Lao People's Democratic Republic. *J Gen Virol* **91**: 949–959
22. Nidom CA et al (2010) Influenza A (H5N1) viruses from pigs, Indonesia. *Emerg Infect Dis* **16**: 1515–1523
23. Watanabe Y, Ibrahim MS, Ellakany HF, Abd El-Hamid HS, Ikuta K (2011) Genetic diversification of H5N1 highly pathogenic avian influenza A virus during replication in wild ducks. *J Gen Virol* **92**: 2105–2110
24. Rappuoli R, Dormitzer PR (2012) Influenza: options to improve pandemic preparation. *Science* **336**: 1531–1533
25. Kilany WH et al (2011) Protective efficacy of H5 inactivated vaccines in meat turkey poulters after challenge with Egyptian variant highly pathogenic avian influenza H5N1 virus. *Vet Microbiol* **150**: 28–34
26. Pang T, Guindon GE (2004) Globalization and risks to health. *EMBO Rep* **5**: S11–S16
27. Weigmann K (2004) Fashion of the times. The emergence and evolution of new research fields is as much determined by scientific interest as it is by social, political and economic pressures. *EMBO Rep* **5**: 1028–1031



Yohei Watanabe [top left] and Kazuyoshi Ikuta [bottom left] are at the Department of Virology, Research Institute for Microbial Diseases, Osaka University, Suita, Osaka, Japan. Madiha S. Ibrahim is at the Department of Microbiology and Immunology, Faculty of Veterinary Medicine, Damanhour University, Damanhour, Egypt. E-mail: nabe@biken.osaka-u.ac.jp

EMBO reports (2013) **14**, 117–122; published online 11 January 2013; doi:10.1038/embor.2012.212



Letter to the Editor

Misinterpretation in virus clearance studies of biological products due to an uncommon discrepancy between cytopathic effects and infectivity of human immunodeficiency virus (HIV)

We report a case of false-positive HIV infectivity detected by the cytopathic effect (CPE) assay, and we present data showing how to confirm such false-positive results. CPE are apparent cellular responses against viral infections, such as morphological changes in cells and apoptosis. The CPE assay is a useful standard method to determine the presence of infectious viruses during process evaluation for biological products as recommended in guidelines for viral clearance studies [1,2]. Characteristic syncytium formation by infection of specific cells, such as C8166 or MT2 cells, with human immunodeficiency virus (HIV), for example LAI, RF, or HTLV-IIIIB strains of HIV-1, has also been established as a sensitive and conventional CPE assay [3–5].

Surprisingly, atypical syncytium-like CPE of infected cells, induced by the filtrate of HIV-spiked samples even after use of a virus removal filter with a pore size of 15 nm (15-nm filter), were observed in our virus clearance study, despite it having been reported that a 15-nm or 35-nm filter can effectively capture intact HIV particles of 80–100 nm in diameter [3,4]. However, two different researchers have also reported similar phenomena (R. Cameron, personal communication). In the following study, we confirmed that these rare syncytium-like CPE can be reproduced experimentally and that non-infectious HIV components of less than 15 nm could penetrate through a 15-nm filter and induce CPE.

The LAI strain of HIV was sonicated twice using a Bioruptor UCD-200TM (CosmoBio, Tokyo, Japan) at 200 W for 10 min (1-min interval) and pre-filtered with PLANOVA™75N (mean pore size, 72 ± 4 nm; Asahi-Kasei Medical, Tokyo, Japan). The resulting disrupted HIV solution, which included both whole HIV particles and their disrupted components, was filtered with PLANOVA™15N (mean pore size, 15 ± 2 nm; Asahi-Kasei Medical) at a constant pressure of 20 kPa at RT, and all of the filtrate was collected as substances that had passed through a 15-nm filter. The disrupted HIV solution contained 5.05 Log_{10} copies/mL of HIV RNA and the concentration of the viral components group-specific antigen p24 of the capsid protein (p24) and envelope glycoprotein (gp120) was 1056.1 ng/mL and 63.5 ng/mL, respectively. Substantial levels of HIV RNA, p24, and gp120 were also detected in the filtrate from a 15-nm filter, with values of 4.19 Log_{10} copies/mL, 1015.1 ng/mL (yield: 96.1%), and 54.1 ng/mL (yield: 85.2%), respectively.

Next, cultured C8166 cells at a concentration of 1.0×10^5 cells/mL were placed in 96-well plates (0.1 mL/well) and 0.1 mL/well of assay sample was added. During the incubation period of 14 days

at 37 °C, 50 μ L of fresh complete medium was added every 3–5 days. Positive CPE appearance was defined by reference to a report by Ongradi et al. [5]. For the immunofluorescence (IF) assay, cultured C8166 cells 14 days post-infection (dpi) fixed in cold acetone were incubated successively with the primary antibody consisting of anti-HIV polyclonal antibody wt0062 derived from HIV patient sera (1:300), and the secondary antibody consisting of anti-human IgG polyclonal antibody labeled with FITC (1:50, Dako, Glostrup, Denmark). After a 14-day incubation with C8166 cells, the disrupted HIV solution induced typical HIV-specific CPE and virus-specific IF signals, correlating with increases in viral gene expression up to 8.27 Log_{10} copies/mL. CPE were also found in the filtrate of a 15-nm filter at low frequencies: three syncytia or multinucleated giant cells were observed in 1.8×10^5 cells/well. However, IF signals and viral RNA were not detected in the culture fluid (Fig. 1).

Therefore, to confirm the presence or absence of infectious viruses, we carried out three subsequent blind passages after the first cultivation of samples with C8166 cells. For the blind passage, 1.0×10^5 cells of cultured C8166 14 dpi and an equal number of naive C8166 cells were seeded in 24-well plates and cultured in 2 mL/well of complete medium at 37 °C. Three blind passages were performed at 3- to 5-day intervals. Treatment with the disrupted HIV solution led to maintenance of or small increases in substantial amounts of HIV RNA and HIV antigens, and typical syncytia and IF signals were observed in every blind passage. C8166 cells treated with the filtrate from a 15-nm filter had no signs of these viral parameters as a negative control (Fig. 1B). These observations indicated that the presence of infectious HIV in the filtrate of a 15-nm filter could be clearly ruled out. This is the first finding that non-infectious HIV components penetrated through a 15-nm filter to induce syncytium-like CPE. The action of the HIV components may involve indirect and complex processes or a mechanism by agents other than a well-known factor, such as gp120, because a long incubation period of 14 days was needed for syncytial formation. While activation of cellular signal transduction and induction of syncytia by HIV envelope protein-expressing cells have been reported [6], further detailed investigation will be needed to clarify this unexplained result.

Notably, syncytium-like CPE induced by non-infectious HIV components could lead to misinterpretation of inactivation or removal abilities in manufacturing processes. If an atypical and/or unreasonable morphological change such as CPE is observed,

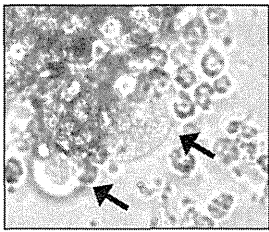
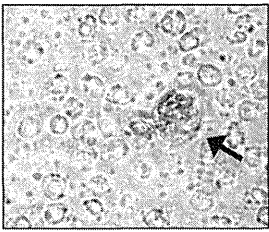
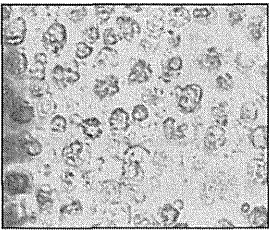
	Disrupted HIV solution	The filtrate of 15-nm	Medium (Negative control)
A			
CPE	++	+	-
IF assay	++	-	-
HIV RNA (Log ₁₀ copies/mL)	8.27	n.d.	n.d.
p24 /gp120 antigen (ng/mL)	337.2 / 5.4	138.9 / 1.1	n.d. / n.d.
B			
CPE	++	-	-
IF assay	++	-	-
HIV RNA (Log ₁₀ copies/mL)	8.46	n.d.	n.d.
p24 /gp120 antigen (ng/mL)	647.1 / 19.0	n.d. / n.d.	n.d. / n.d.

Fig. 1. Images of morphological changes (phase contrast) and results of IF signals, as well as amounts of HIV RNA, p24 antigen, and gp120 after incubation with disrupted HIV solution, the filtrate of a 15-nm filter, and medium as assay samples, respectively. The arrows represent a syncytium-like typical morphological change or atypical morphological change. (A) The results of CPE, IF signals in cultured cells, and amounts of HIV RNA, p24, and gp120 antigen in culture fluid (at 14 dpi). (B) The results after three serial blind passages. The cultured cells (at 14 dpi) described above were subsequently used for blind passage. ++ = strongly positive, + = positive/weakly positive, - = negative, n.d. = not detected.

careful interpretation of the phenomenon is needed. Consequently, CPE may be induced both by intact HIV and by noninfectious components, and IF assay and blind passages are useful tools for specific identification of infectious HIV, even if samples coexist with such non-infectious components that cause morphological changes in cells.

Conflict of interest

We declare that we have no conflicts of interest. This work was conducted on the basis of collaborative research projects between Osaka University, BioReliance Ltd., Asahi Kasei Medical Co., Ltd., and Benesis Corporation, and the research fund used in this study was provided by Benesis Corporation. Takeru Urayama and Mikihiro Yunoki are employees of Benesis Corporation (Japan Blood Products Organization).

Acknowledgments

The authors thank Ms. Tomoko Kotani of BioReliance for helpful discussions and kind support.

References

- [1] Ministry of Health, Labour and Welfare (MHLW). Guidelines on the establishment of viral safety for plasma fraction products. Ref. No. 1047. Tokyo: Pharmaceutical and Food Safety Bureau; 30 August 1999 (in Japanese).
- [2] International Conference on Harmonization of Technical Requirements for Registration of Pharmaceuticals for Human Use (ICH). Viral safety evaluation of biotechnology products derived from cell line of human or animal origin. Harmonised Tripartite Guideline Q5A(R1); 23 September 1999.

- [3] Terpstra FG, Kleijn M, Koenderman AHL, Over J, van Engelenburg FAC, Schuitemaker H, et al. Viral safety of C1-inhibitor NF. *Biologicals* 2007;35: 173–81.
- [4] Roberts PL, Feldman P, Crombie D, Walker C, Lowery K. Virus removal from factor IX by filtration: validation of the integrity test and effect of manufacturing process conditions. *Biologicals* 2010;38:303–10.
- [5] Ongradi J, Laird HM, Szilagyl JF, Horvath A, Bendinelli M. Unique morphological alterations of the HTLV-1 transformed C8166 cells by infection with HIV-1. *Pathol Oncol Res* 2000;6:27–37.
- [6] Michalski CJ, Li Y, Kang CY. Induction of cytopathic effects and apoptosis in *Spo-doptera frugiperda* cells by the HIV-1 Env glycoprotein signal peptide. *Virus Genes* 2010;41:341–50.

Takeru Urayama*¹

Osaka Research Laboratory, Research and Development Division,
Benesis Corporation, 3-16-89 Kashima, Yodogawa-ku, Osaka-shi,
Osaka 532-8505, Japan

Department of Virology, Research Institute for Microbial Diseases,
Osaka University, 3-1 Yamadaoka, Suita, Osaka 565-0871,
Japan

Roslyn Cameron

BioReliance Ltd., Innovation Park, Hillfoots Road, Stirling, FK9 4NF,
Scotland, United Kingdom

Tetsuo Sato

Science & Technology Department, Planova Division, Asahi Kasei
Medical Co., Ltd., 1-105 Kanda Jinbocho, Chiyoda-ku,
Tokyo 101-8101, Japan

Mikihiro Yunoki¹

Osaka Research Laboratory, Research and Development Division,
Benesis Corporation, 3-16-89 Kashima, Yodogawa-ku, Osaka-shi,
Osaka 532-8505, Japan